Conducting Hydrogel-Based Neural Biointerfacing Technologies

Pei Zhang, Yifan Yang, Zhaobo Li, Yu Xue, Fucheng Wang, Liangjie Shan, Yafei Wang, Xuetao Shi,* Kai Wu,* and Ji Liu*

Neural biointerfacing, enabling direct communication between neural systems and external devices, holds great promises for applications in brain machine interfaces, neural prosthetics, and neuromodulation. However, current neural electronics made of conventional rigid materials are challenged by their inherent mechanical mismatch with the neural tissues. Hydrogel bioelectronics, with mechanical properties compatible with the neural tissues, represent an alternative to these limitations and enable the next-generation neural biointerfacing technology. Here, an overview of cutting-edge research on conducting hydrogels (CHs) bioelectronics for neural biointerfacing development, emphasizing material design principles, manufacturing techniques, essential requirements, and their corresponding application scenarios is presented. Future challenges and potential directions regarding CHs-based neural biointerfacing technologies, including long-term reliability, multimodal hydrogel bioelectronics for closed-loop system and wireless power supply system, are raised. It is believed that this review will serve as a valuable resource for further advancement and implementation of next-generation neural biointerfacing technology.

P. Zhang, Y. Xue, F. Wang, L. Shan, Y. Wang, J. Liu
Department of Mechanical and Energy Engineering
Southern University of Science and Technology
Shenzhen 518055, China
E-mail: liuj9@sustech.edu.cn

Y. Yang, X. Shi
School of Materials Science and Engineering
South China University of Technology
Guangzhou 510640, China
E-mail: shxt@scut.edu.cn

Y. Yang, X. Shi, K. Wu
National Engineering Research Centre for Tissue Restoration
and Reconstruction
South China University of Technology
Guangzhou 510006, China
E-mail: kaiwu@scut.edu.cn

Z. Li, F. Wang, K. Wu
School of Biomedical Sciences and Engineering
South China University of Technology, Guangzhou International Campus
Guangzhou 511442, China

X. Shi, K. Wu
Key Laboratory of Biomedical Engineering of Guangdong Province
South China University of Technology
Guangzhou 510006, China
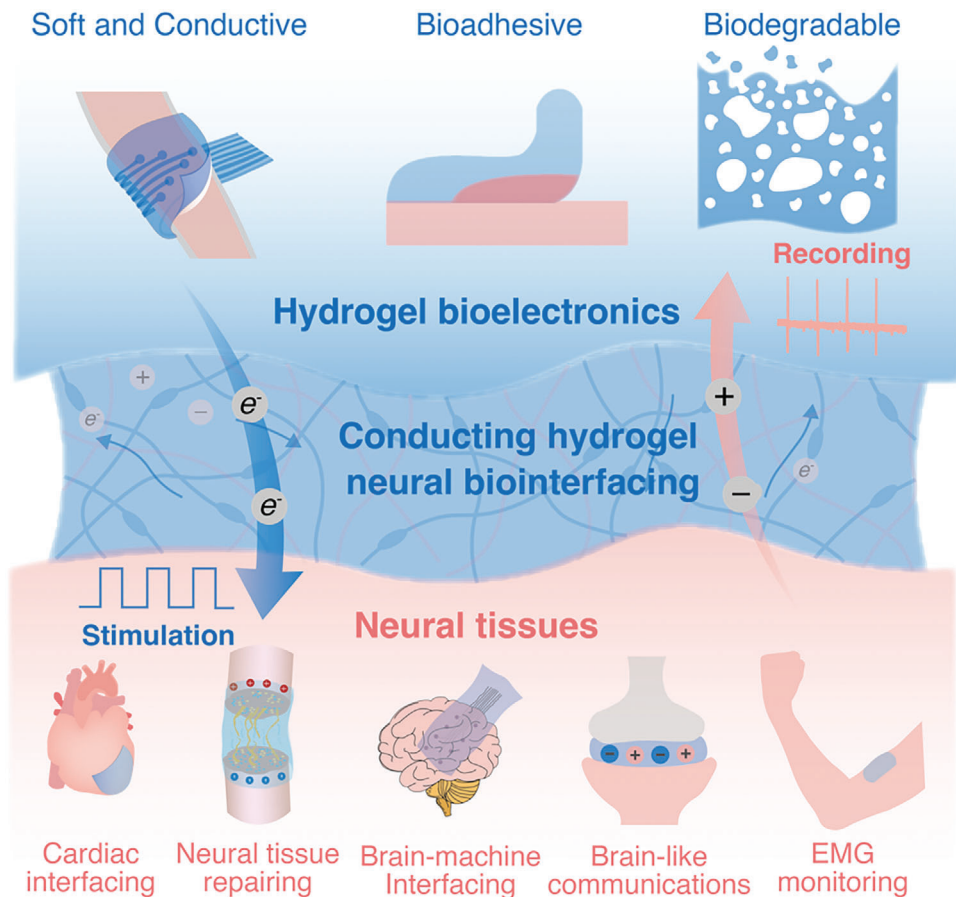
1. Introduction

Neural biointerfacing is essential for effectively bridging the bidirectional communication channels between neural systems and external devices, which remains a central challenge in neural engineering.[1] Such biointerfacing technology is playing a crucial role in applications such as brain-machine interfaces (BMIs),[2] neural prosthetics and neuromodulation therapies for conditions like Parkinson's disease,[3] Alzheimer's disease,[4] and major depressive disorders.[5] The primary function of neural biointerfacing is to facilitate communication between neural tissues and bioelectronic devices by recording the neural activities and/or delivering stimulation, such as optical,[6] chemical,[7] or electrical triggers.[8] Over the past decades, Michigan-type[9] and Utah-type[10] microelectrode arrays have been widely utilized to significantly facilitate bidirectional communication in neural interfacing, enabling precise recording and stimulation of neural activities for various neural engineering applications. However, conventional materials used in neural biointerfacing, such as metals or rigid semiconductors, exhibit high modulus ($\approx$GPa) and fail to provide mechanical ($\approx$Pa) and biological compliance for long-term neural implantation.[11] Such dramatic mismatch between the rigid neural electronics and soft yet wet, neural tissues can result in tissue damage, chronic inflammation, and signal distortion, thus limiting the performance and lifespan of the implantable devices.[12] Recent studies have shown that engineering bulky and rigid metallic materials to mesh[13] or serpentine structure[14] with ultrathin thickness, could slightly mitigate the mechanical mismatch for metallic bioelectronics. In addition, incorporating conducting fillers into intrinsically stretchable substrates[15] can also be exploited as an alternative to improve the interfacial mismatch for the neurals-electrode biointerfacing. Long-term neural implantation of such bioelectrodes are still facing challenges, such as inflammatory response, fibrosis encapsulation, as well as gradually deteriorated performance.[16]

Hydrogels have emerged as promising alternatives to traditional rigid materials for electronic biointerfacing technologies.[17] Due to the intrinsic similarity in chemical and structural properties between hydrogel materials and biological tissues, such as high-water content, mechanical softness,

**ADVANCED
SCIENCE NEWS**

www.advancedsciencenews.com

**ADVANCED
FUNCTIONAL
MATERIALS**

www.afm-journal.de

Figure 1. CHs-based neural biointerfacing. Schematic illustration for the features of hydrogel bioelectronics (i.e., softness, ion/electron conductivity, bioadhesion, biocompatibility, and biodegradability) for diverse neural biointerfacing applications (i.e., cardiac interfacing, neural tissue repairing, brain-machine interface, brain-like communication, and EMG monitoring). The CHs serves as a bridge between the bioelectronics and neural tissues, enabling both electrical stimulation and neural signal recording.

hydrophilic essence, and superior biocompatibility, hydrogels have been widely utilized in bioelectronics,[18] tissue engineering,[19] and biomedicines,[20] *etc.* For instance, hydrogel-based neural electronics could be imparted with mechanical modulus (≈kPa) similar to the neural tissues.[21] The mechanical compatibility with neural tissues not only minimizes the mechanical damages and chronic inflammations upon implantation but also improves the long-term stability of the neural biointerfacing.[22] Conducting hydrogels (CHs), with superior ion- and/or electron conductivity, are highly promising electrode materials for electrophysiological signal recording and electrical stimulation. In light of their inherent biocompatibility and mechanical compliance, long-term implantation of CHs-based bioelectronics could effectively minimize the inflammatory and immune responses in the surrounding tissues.[11] Furthermore, most polymer hydrogel networks could be readily engineered with desirable biodegradability,[23] which are essential for minimizing the risk of immune responses and ensuring reliable integration with the neural tissues.

Recent reviews on neural biointerfacing have mainly focused on BMIs,[8c,24] rigid electronics,[25] and flexible conducting coatings[26] for neural devices. Even though functional hydrogels have been in-depth reviewed as promising biointerfac-

ing materials,[18b,27] CHs-based electronics used for neural biointerfacing have rarely been summarized. Herein, this review will focus on the recent developments of CHs for neural biointerfacing, ranging from the general design principles, manufacturing technologies for CHs, as well as key requirements and application scenarios in neural biointerfacing, as outlined in **Figure 1**. We first present an overview on typical strategies to functionalize hydrogels with superior conductivity, including incorporating metallic nanoparticles, ion doping, and intrinsically conducting polymers hydrogels. Subsequently, we discuss the manufacturing technologies for CHs-based bioelectronics, including photolithography, templating, screen printing, laser-assisted patterning, and extrusion-based printing, especially focusing on the fundamental principles and processing precision. Importantly, we also summarize the key requirements of hydrogel electronics used for neural biointerfacing, such as mechanical compliance, interface adhesion, biodegradability, and long-term stability. We then provide an overview of hydrogel electronics applications in cardiac interfacing, neural tissue repairing, BMIs, brain-like neuronal communication, and electromyographic (EMG) monitoring. Finally, we discuss the future implications and challenges of next-generation hydrogel-based neural biointerfacing, including long-term reliability, multimodal hydrogel bioelectronics for

**ADVANCED
SCIENCE NEWS**

www.advancedsciencenews.com

**ADVANCED
FUNCTIONAL
MATERIALS**

www.afm-journal.de

closed-loop system and wireless power supply system. Such advancements hold great potential for revolutionizing the bioelectronics and neural biointerfacing fields, leading to sophisticated and seamless biointerfacing between neural tissues and hydrogel bioelectronics.

2. Design Principles of CHs for Bioelectronics
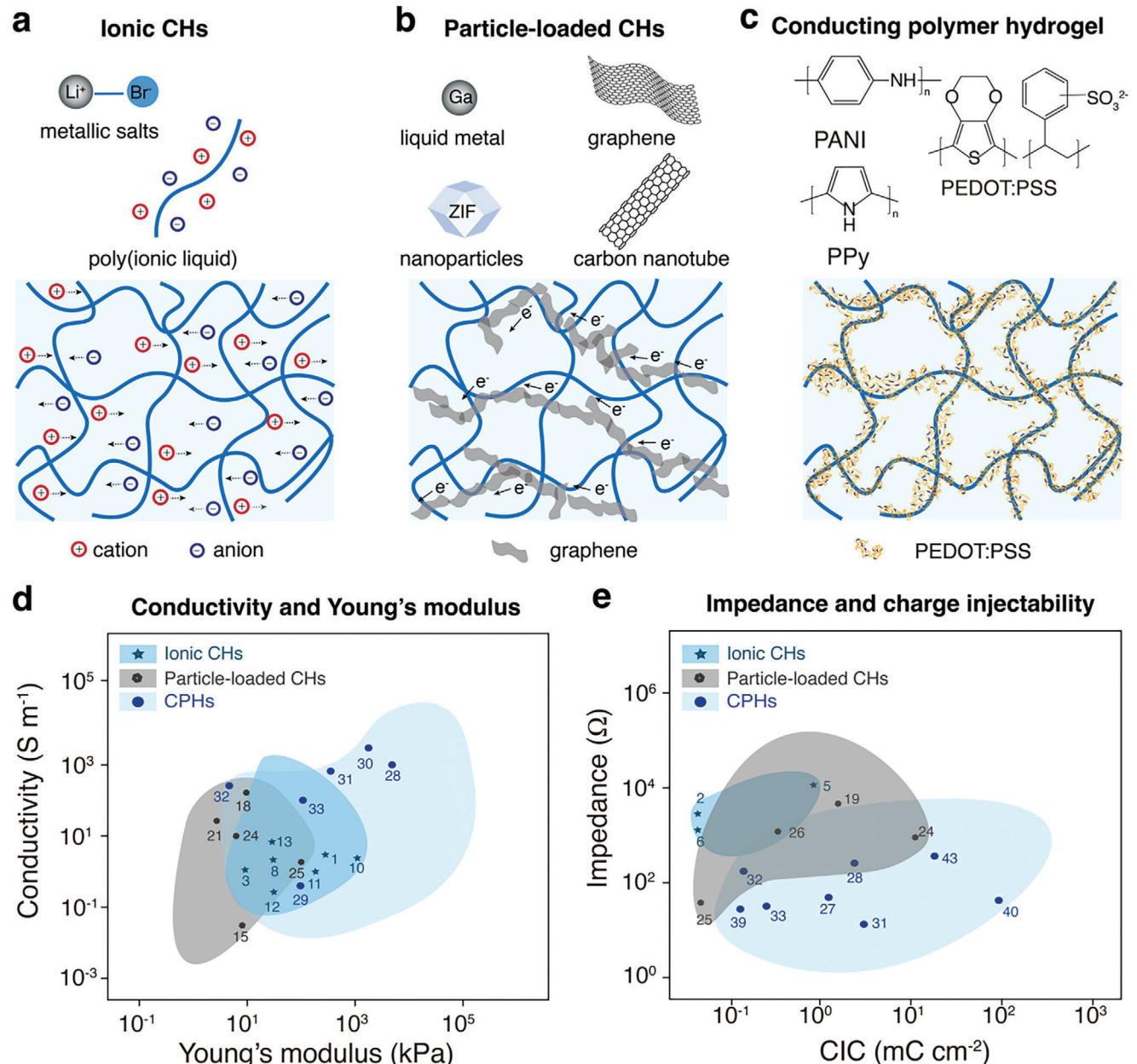
The inherent mechanical mismatch between traditional rigid electronics (e.g., Utah electrode, with a modulus exceeding 100 GPa) and neural tissues (with a modulus below 100 kPa)[28] poses significant challenges for maintaining a robust neural biointerfacing over time. This mismatch often leads to scar formation and inflammatory responses, severely compromising functionalities of the neural electronics,[16,29] representing a substantial obstacle for the advancement in neural biointerfacing technologies. CHs, a new class of flexible, stretchable, and conducting materials, are emerging as ideal candidates for bridging the interface between human tissues and electronic devices. Hydrogels are polymeric materials with a 3D network structure formed through the crosslinking of polymer chains. These materials have the ability to absorb and retain a large amount of water without dissolving.[17f] The CHs electrode is typically consisted of conducting modalities and a hydrogel network. The hydrogel polymer provides the structural framework, while the conducting medium ensures electrical conductivity. According to the methods of incorporating conducting modalities, CHs can be classified into three main categories: i) incorporating conducting ions, such as inorganic salts,[30] ionic liquids, and polyelectrolytes[31] (**Figure 2a**); ii) embedding conducting particles, such as carbon-based conducting materials (e.g., carbon nanotubes (CNTs),[32] graphene,[33] and carbon fibers), metal nanoparticles[34] (e.g., metal nanowires,[35] metallic nanoparticles, and liquid metals[36]), or other conducting particles (e.g., MXene[37] and metal-organic frameworks[38]) (Figure 2b); and iii) integrating intrinsically conducting polymers (e.g., polypyrrole (PPy),[39] polyaniline (PANi), and poly(3,4-ethylenedioxythiophene) (PEDOT)),[40] in order to fabricate CHs networks (Figure 2c). In this section, we summarize the design principles, advantages, and limitations of various design and fabrication strategies for CHs.

Ionic CHs rely on the movement of ions within the hydrogel network to effectively transmit the electrical signals (Figure 2a). The ionic CHs exhibit a conductivity range of 10^{-1} to 10^3 S m^{-1} and a Young's modulus range of 10 to 10^3 kPa (Figure 2d and Table S1, Supporting Information). The addition of ions enhances the conductivity of the hydrogels while preserving its flexibility and elasticity, closely mimicking the natural transmission of electrical signals in biological systems.[30] This similarity allows ionic CHs to adapt effectively to the dynamic physiological environments. For instance, using a salting-out approach, polyvinyl alcohol (PVA)-based hydrogels can achieve a high stress (1.3 MPa) and strain (975%), while a porous structure with a rich ionic environment can significantly enhance the ionic conductivity (up to 3.4 S m^{-1}).[41] However, the performance of ionic CHs was highly sensitive to changes in the ion concentration and water content. Upon reaching a 30% CaCl$_2$ concentration, the PVA hydrogel exhibited a 39% enhancement in strength, a three-fold increase in tensile strength, and a three-fold elevation

in conductivity relative to the CaCl$_2$-free hydrogel. Additionally, the modulus of the hydrogel was augmented by roughly four times.[42] Impedance and charge injection capacity (*CIC*) influence the performance of CHs from two key perspectives: electrical signal transmission efficiency and electrochemical activity. Low impedance enhances signal transmission and interface matching, while high *CIC* improves the effectiveness and durability of the material in stimulation or storage applications. The impedance of ionic CHs ranges from 10^2 to 10^4 Ω, while their *CIC* spans from 10^{-3} to 1 mC cm^{-2} (Figure 2e and Table S1, Supporting Information). Water loss or fluctuations in environmental ion levels can destabilize the conductivity. Given the limited mobility of ions, the ionic conductivity is typically low (10^{-1} to 10^3 S m^{-1}),[42b] and ions migration or dissipation over time can further decrease the ionic conductivity, thus deteriorating the performance of ionic CHs-based electronics.[44]

In contrast, particle-loaded CHs primarily rely on electronic conduction. Conducting nano/microparticles, such as carbon-based materials or metallic nanoparticles, exhibit excellent electronic conductivity, resulting in extremely high conductivity (i.e., 370 S cm^{-1})[43] and long-term robustness. The conductivity and mechanical properties of these hydrogels can be easily adjusted by modifying the type, concentration, shape, and distribution of the conducting particles. For example, when 0.2 mg mL^{-1} of GO was incorporated into a GelMA hydrogel networks, the conductivity and elasticity increased by seven-fold and two-fold, respectively, while the impedance was reduced to just one-twentieth of its original value.[33] The impedance of such hydrogels typically ranges from 10 to 10^5 Ω, with *CIC* spanning 10^{-2} to 50 mC cm^{-2} (Figure 2e and Table S1, Supporting Information).[27a] Filling conducting particles could also enhance the mechanical strength and toughness of the hydrogel network, and also increase in rigidity, with Young's modulus values ranging from 1 to 10^2 kPa. (Figure 2d and Table S1, Supporting Information).[27a,45] Despite recent advancements, these strategies are also facing some intrinsic limitations. Specifically, increasing the fraction of conducting particles to enhance the conductivity may compromise the internal network's cross-linking, leading to increased brittleness and reduced mechanical durability.[46] Additionally, non-homogeneous distribution of conducting particles can also cause localized conductivity variations, potentially affecting overall performance.
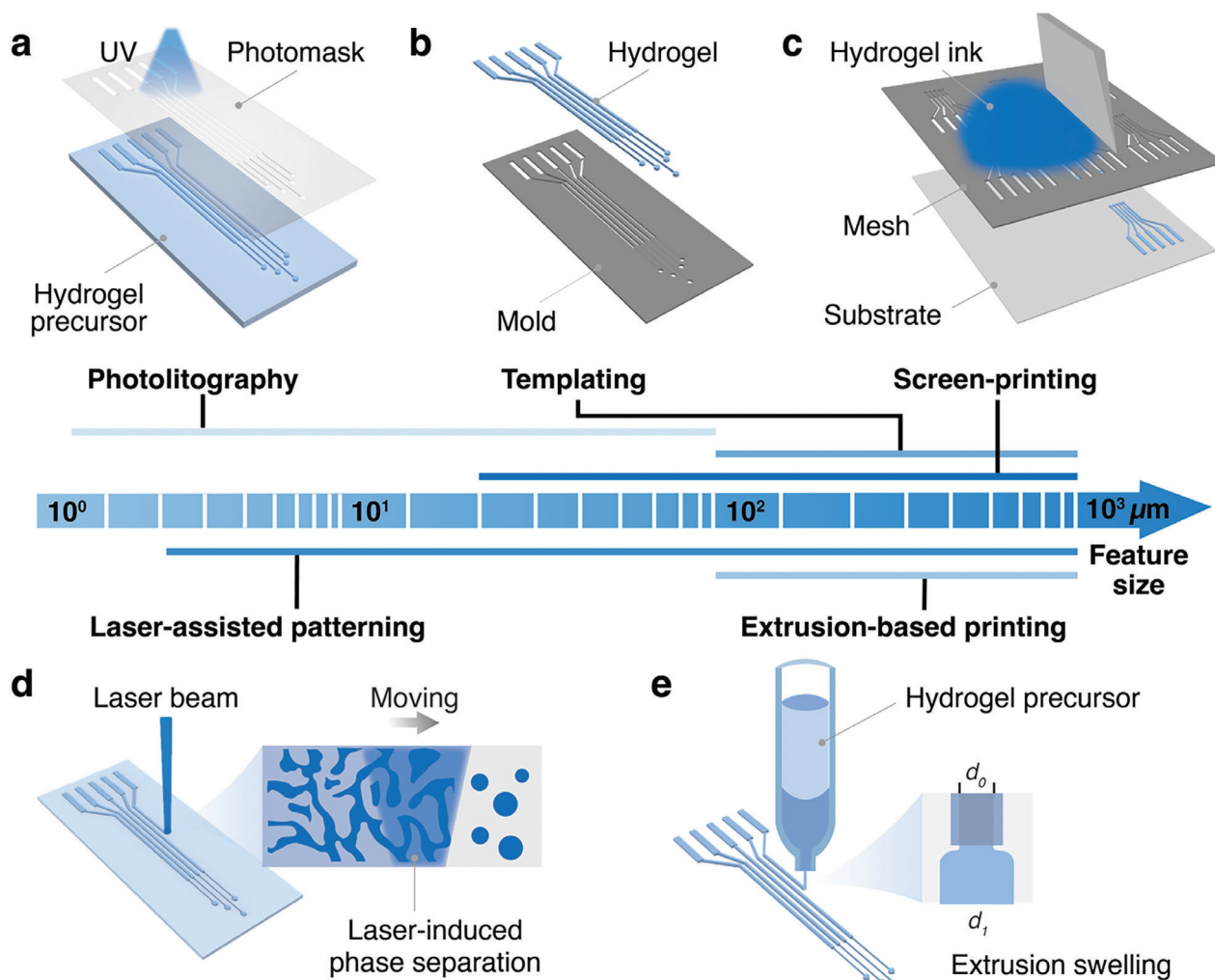
Conducting polymers (CPs) are π-conjugated polymers, where electrons are confined within a robust polymer backbone, and the delocalized π-electrons can migrate freely within the π-conjugated structure, forming an efficient charge conduction pathway (Figure 2c). This charge conduction enables high conductivity and signal stability.[47] Conducting polymer hydrogels (CPHs) exhibit excellent conductivity, making them highly suitable for recording and transmitting neural signals with enhanced sensitivity and stability, while also minimizing inflammatory and immune responses in the surrounding tissues. Commercially available PEDOT: PSS suspension, such as Clevios pH1000, generally exhibit low conductivity (<1 S cm^{-1}),[40b] and pure PEDOT: PSS hydrogel made from these polymer suspensions have a conductivity of ≈40 S cm^{-1}, but exhibit poor mechanical properties (i.e., Young's modulus ≈2 MPa, strain < 10%[40a]), making them unsuitable for fabricating bioelectronics. Various strategies, such as doping, structural design, and chemical modifications, have

ADVANCED
SCIENCE NEWS

www.advancedsciencenews.com

ADVANCED
FUNCTIONAL
MATERIALS

www.afm-journal.de

Figure 2. Design principles for CHs. CHs can be categorized into a) ion-based, b) particle-based, and c) conducting polymer hydrogels. d) Compared chart by plotting Young's modulus and conductivity for ionic CHs, particle-loaded CHs and conducting polymer hydrogels. e) Comparison chart by plotting impedance and *CIC* for ionic CHs, particle-loaded CHs and conducting polymer hydrogels. The points in the d) and e) represent actual data points, with their specific values and corresponding references provided in Table S1 (Supporting Information). The boundary ranges are determined based on other data from Table S1 (Supporting Information) and corresponding references.[27a,b]

been utilized to increase the conductivity (ranging from 1 S cm^{-1} to 10^3 S cm^{-1}) without sacrificing the mechanical compliance the Young's modulus of 10 kPa–10 MPa) (Figure 2d and Table S1, Supporting Information). By adding dopants, the orientation of the PEDOT framework and local ordering can be tailored, accompanied with tuned phase separation, thereby enhancing the conductivity and reducing the impedance.[48] For example, the addition of small molecules or functionalized polymer chains can facilitate the ordered stacking of PEDOT chains. Dopants such

as DMSO,[88] salts,[49] or ionic liquids, can influence the interactions between the conducting polymer chains and the aqueous phase, promote phase separation between PEDOT and PSS, and then facilitate the formation of locally ordered PEDOT domains, thereby directly improving the conductivity of the CPHs. For example, organic ions, such as sodium dodecylbenzene sulfonate (SDBS) or ionic liquids, could effectively soften the PSS chains and enhance the PEDOT connectivity, thereby increasing the overall conductivity up to 4000 S cm^{-1}.[48] On the other hand,
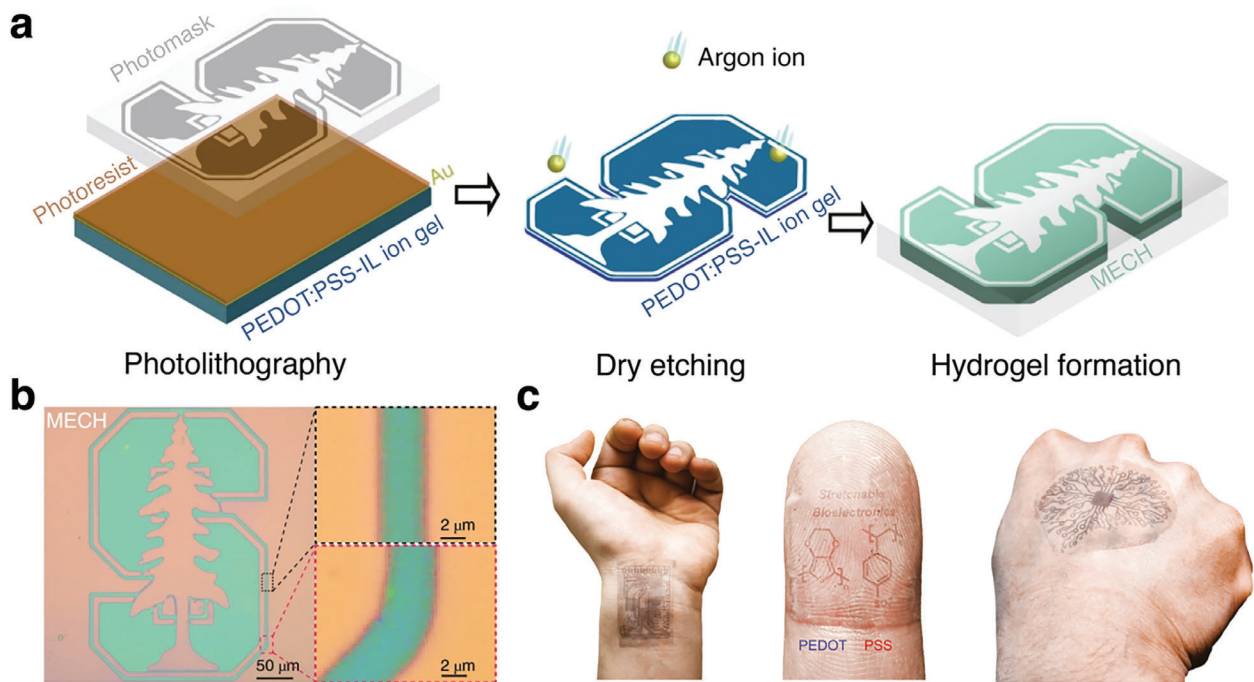
Figure 3. Manufacturing strategies for CHs-based bioelectronics. Hydrogel bioelectronics could be readily fabricated through various strategies. a) Photolithography. By exposing a hydrogel precursor to ultraviolet (UV) light through a photomask, a high-resolution pattern could be formed upon etching the photoresist layer. b) Templating. By filling a pre-designed mold with hydrogel precursors, patterned hydrogel bioelectrodes could be obtained upon curing the precursors. c) Screen printing. By transferring the CHs inks onto a substrate using a pre-patterned screen, the hydrogel inks could precisely deposit onto the substrates with pre-designed patterns. d) Laser-assisted patterning. The focused laser beam could induce the in-situ phase separation of CHs, resulting in hydrogels with pre-designed patterns. e) Extrusion-based printing. A shear-thinning CHs-based inks are extruded throughout a nozzle, immediately solidify and form pre-designed patterns and/or 3D geometries. With controlled extrusion swelling (d_1/d_0), the fabrication resolution could be tailored.

inorganic ions, such as metal halides, could promote electron mobility through a charge-exchange mechanism, further stabilizing the conducting pathways, resulting in electron conductivity as high as 540 S cm^{-1}.[43b] Further removal of the ionic liquid additives through water exchange helps maintain the conductivity (i.e., 47 S cm^{-1}) and impedance stability, as well as superior mechanical compliance (i.e., Young's modulus of 32 kPa).[49] To achieve a balance between conductivity and flexibility, multilayer structures that combine mechanically robust polymers with CPs can be used. The impedance of such CPHs ranges from 1 to 10^4 Ω, while their *CIC* spans from 10^{-1} to 6 × 10^2 mC cm^{-2} (Figure 2e and Table S1, Supporting Information).[27a] Additional optimizations can be achieved by incorporating co-monomers or through functional chemical modifications. For example, by incorporating 4-vinyl pyridine within the long-chain polymer poly

(styrene sulfonate-*co*-4-vinyl pyridine),[8c] it allowed for chemical crosslinking of the PSS main chains, thus effectively toughening the PEDOT: PSS CHs networks, as well as long-term stability.

3. Manufacturing Strategies of CHs-Based Bioelectronics

The high-water content and soft nature of hydrogel materials render high-temperature and high-vacuum processing techniques, which are commonly used for traditional rigid electronics, unsuitable for hydrogel-based electronics fabrication. As shown in **Figure 3**, this section will present an overview of the advanced manufacturing strategies used for the fabrication of hydrogel bioelectronics, including photolithography, templating, screen printing, laser-assisted patterning, and extrusion-based printing.

**ADVANCED
SCIENCE NEWS**

www.advancedsciencenews.com

**ADVANCED
FUNCTIONAL
MATERIALS**

www.afm-journal.de

Figure 4. Photolithographically patterned CHs-based bioelectrodes. a) Schematic diagram of photolithography process. Photolithography was applied to PEDOT:PSS–ionic liquid (IL) ion gel using an Au hard mask. The micropattern was then transferred onto the ion gel through dry etching. Finally, the patterned ion gel underwent transformation via water exchange. Reproduced with permission.[49] Copyright 2019, Springer Nature. b) Micropatterned electrically conducting hydrogel (MECH) with feature sizes down to 1.5 µm. Reproduced with permission.[49] Copyright 2019, Springer Nature. c) Photographic images of micropatterned PEDOT:PSS hydrogel. Reproduced with permission.[53] Copyright 2022, AAAS.

3.1. Photolithography

Fabrication of hydrogel bioelectronics via photolithography involves coating a hydrogel precursor onto a substrate, exposing it to UV light through a photomask to create a predefined pattern (Figure 3a), followed by etching the photoresist layer to obtain the hydrogel patterns. Normally, photolithography is applied to inorganic (i.e., SiO_2/Si,[50] ZnO[51]) or rigid organic materials (i.e., polymethyl methacrylate (PMMA) or acrylonitrile butadiene styrene (ABS)[52]) for high-resolution patterned electronics, with a resolution below 400 nm. Due to the high-water content of hydrogels and tendency to swell in direct contact with the precursor solution, overexposure between adjacent structures results in limited resolution ($\approx$100 µm). As a result, conventional photolithography encounters significant challenges in producing high-precision and direct patterning of CHs. Bao et al.[49] developed a CHs-based electrode with 5 µm resolution by applying traditional photolithographic patterning to an ion gel (PEDOT: PSS-IL ion gel), which was then converted into a micropatterned CHs (**Figure** 4a). Uncontrollable swelling of the micropatterned CHs could be solved by solvent exchange.[49] A fluorinated elastomeric photoresist, derived from dimethacrylate-functionalized perfluoropolyether (PFPE-DMA), was designed to resist the swelling from ionic liquid-modified PEDOT: PSS, with organic solvents used during the photolithography. Once the precursor was cured through UV exposure, the as-obtained patterns exhibited high elasticity, flexibility, and chemical stability in most solvents. The CHs was sandwiched between PFPE-DMA photoresists and photolithographically patterned, while Au-based

hard mask was used during etching. The PFPE-DMA photoresists could be directly photopatterned with a feature size as small as 1.5 µm (Figure 4b,c).[49,53] However, due to the anisotropic swelling (swelling ratio of $\approx$2.1), the effective resolution reduced from 1.5 to 20 µm. Furthermore, the patterned CHs prepared from photolithography could also be directly used as replication for soft lithography. Zhu et al.[54] reported a photo responsive hydrogel (acrylamide/azobenzene-cyclodextrin, AM/AZO-CD) patterned by photolithography, and then used as a reusable replicated mould for fabricating micropatterned polydimethylsiloxane (PDMS) with surface smoothness of $\approx$3.4 nm and minimum feature size of 40 µm. In addition, grayscale photolithography combined digital light processing can be used to fabricate micropatterned array of hydrogel electronics with different heights within one step.[54] Compared with other fabrication methods, photolithography enables the creation of hydrogel bioelectronics with extremely small features (down to several micrometers). However, it is limited to producing 2D plannar patterns, while change in electrode patterns requires the use a newly-designed photomask, making the process less efficient and cost-effective. Additionally, the light source used in photolithography may damage the hydrogel networks, particularly for those systems containing living active components, such as enzymes and bacteria.

3.2. Templating

Templating is one of the most effective and universal strategies to fabricate hydrogel electronics among all these methods.

The direct fabrication of CHs bioelectronics through templating involves pouring CHs precursors into a pre-designed mold (Figure 3b), ensuring accurate alignment with the desired patterns. Afterwards, the hydrogel precursor undergoes in situ curing, where chemical crosslinking, UV polymerization, air drying or other curing methods solidify the CHs networks. The final hydrogel electronics patterns are obtained upon subsequent removal of the mold. Templating accommodates hydrogel precursors of various rheological attributes (i.e., flowing fluids or viscous slurries), and supports multiple solidification strategies (i.e., air drying, UV or thermal curing).[55] Typically, micropatterned molds are produced using laser cutting or 3D printing. Poly (methyl methacrylate) (PMMA) and polyethylene terephthalate (PET) are commonly used as substrates for creating moulds through laser cutting. Due to their high transparency, PMMA and PET moulds allow lasers to penetrate easily, enabling the processing of high-resolution moulds ($\approx$200 μm),[56] and the hydrogels can be easily demoulded in light of the hydrophobic surface of PMMA and PET. For example, He et al.[57] prepared hydrogel electronics with multi-channel conducting arrays through templating, and the hydrogel precursors were composed of PVA (15 wt.%) and PPy (10 wt.%–30 wt.%), with conductivity varying from 1 to 100 S cm^{-1}. Specifically, waterproof tapes with customized patterns, such as bauhinia and 12-channel conduits, were used as a mask to cover the PVA hydrogel membrane (250 μm thickness), and only the areas exposed by the mask were treated with pyrrole (Py) and FeCl$_3$ solutions. Thus, PPy was selectively incorporated into PVA hydrogels with patterns. However, this template mask method is limited to feature sizes at the millimeter scale. Furthermore, 3D printed molds, with more complicated patterns than laser cutting moulds, are also widely fabricated using acrylate, polylactic acid (PLA), or polycarbonate (PC). For example, Park et al.[58] prepared a hydrogel electrode based on liquid metal by transfer printing using a 3D-printed mould. The mould with integrated multichannel circuits was fabricated using a 3D-printed acrylic resin. In addition to laser cutting and 3D printing, molds with 3D micropyramid structures were also developed for replicating and patterning CHs electronics.[59] These hydrogel electronics incorporate 3D gradient microstructures, enabling high precision and extensive contact sensing capabilities. Overall, templating is one of the most commonly used methods for fabricating hydrogel electronics, offering broad material versatility with minimal restrictions on material systems. However, the limitations of mold size and challenges in detachment hinder the large-scale production and high-precision fabrication of hydrogel bioelectronics. Furthermore, similar to photolithography, templating necessitates replacing the mold to modify the pattern of hydrogel bioelectronics, reducing its cost-effectiveness.

3.3. Screen Printing
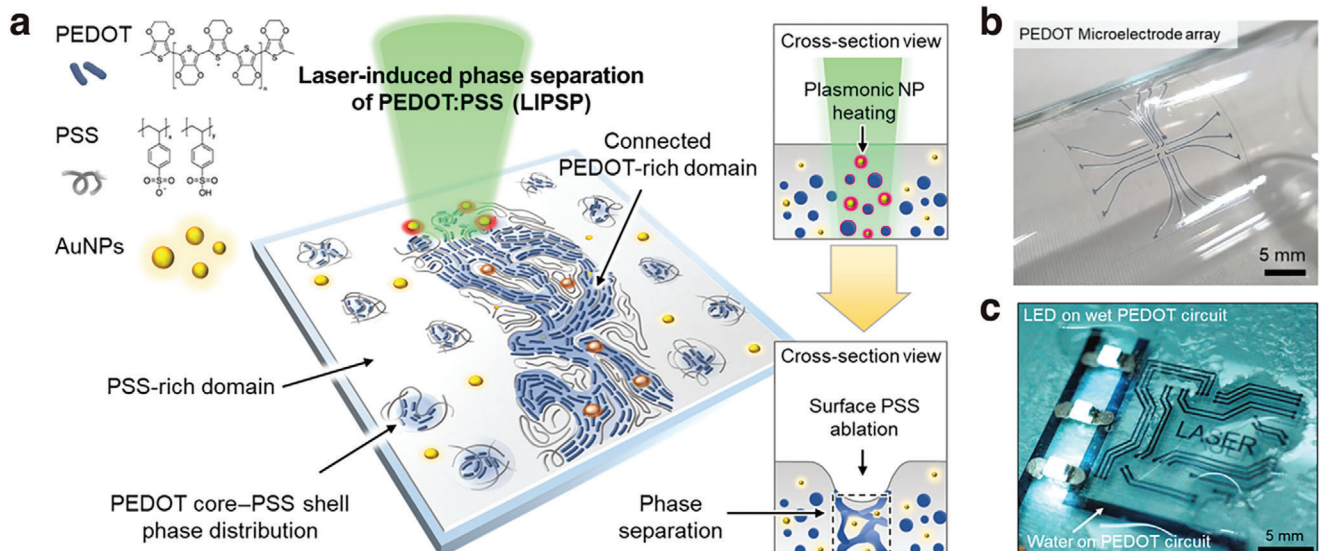
Screen printing involves transferring CHs inks onto a substrate using a pre-patterned screen (Figure 3c), which serves as a stencil to define the desired patterns. A blade, or squeegee, is used to spread the CHs inks across the screen, filling the open areas and depositing the inks precisely. The pressure from the blade ensures even distribution of the ink, while the screen design guarantees accurate pattern transfer onto the substrate. Subsequent curing or drying solidifies the inks and form the final printed structure.[60] Generally, inks used in screen printing exhibit two key rheological properties: shear thinning, where viscosity decreases with increasing shear rate, and rapid shear recovery, where viscosity quickly restores after the removal of shear stress. For instance, Michael et al.[61] developed a screen-printable CHs-based on 15 wt.% polyacrylamide (PAM) and 4 wt.% PEDOT: PSS with high viscosity ($\approx$10^4 Pa s) and a shear thinning behaviour (i.e., viscosity decreases from 10^4 to 1 Pa s upon the increase of shearing rate from 10^{-2} to 10^2 rad s^{-1}). In PAM/PEDOT: PSS ink, the influence of PAM on viscosity is minimal, with viscosity primarily determined by the concentration of PEDOT: PSS. Upon curing the CHs, PEDOT: PSS remains physically entangled within the PAM networks, serving as the conducting pathway, while PAM undergoes cross-linking to form a semi-interpenetrating network with PEDOT: PSS.[61] Beyond the CHs inks utilized in screen printing, design of the screen and the surface properties of the substrate also play critical roles in high-resolution screen-printing. Commonly used screens are made from PET, polyurethane (PU), or PDMS substrates, which are hydrophobic and can be easily detached and separated from CHs. The screens are patterned using laser cutting, achieving resolutions down to hundreds of micrometres. The adhesion between CHs and the substrate can be finely tuned through surface treatments, such as chemical modification with acryloyl groups, to increase the hydrophilicity and improve interface compatibility.[61] Moreover, hydrogel electronics composed of two or more functional materials can be fabricated through multiple screen-printing process, thus allowing for patterns with high complexity.[62] Screen printing for preparing hydrogel bioelectronics offers the advantage of mass production. However, for CHs patterns with extremely low thickness, detaching of the screen is always accoamnied by sample damage, which poses a significant challenge.

3.4. Laser-Assisted Patterning

Laser processing, a non-contact technique, has been recognized as a versatile tool for processing almost all type of materials (e.g., metal, glass, and polymer). This technology uses high-energy-density laser ablation for material processing, offering exceptionally high precision and control in fabrication. When used for patterning CHs electronics, a well-focused laser beam is employed to precisely tailor and shape the hydrogel substrates, enabling the creation of intricate patterns and structures (Figure 3d). When the laser irradiates the surface of the CHs films, the thermal energy causes the material sublimation along the created micropatterns or micro-channels.[63] Consequently, the localized heating on the hydrogel surface poses a crucial impact on processing resolution and quality due to potential thermal damage. The laser beam radius and intensity are adjusted to control the width of the patterns.

For example, Rikuto et al. fabricated conducting agarose hydrogel by laser-based graphitization with processing width ranging from 30 to 1000 μm.[65] Specifically, the manufacturing resolution varied from 30 to 110 μm with the laser intensity increased from 25 to 100 mW. In addition to thermal sublimation of
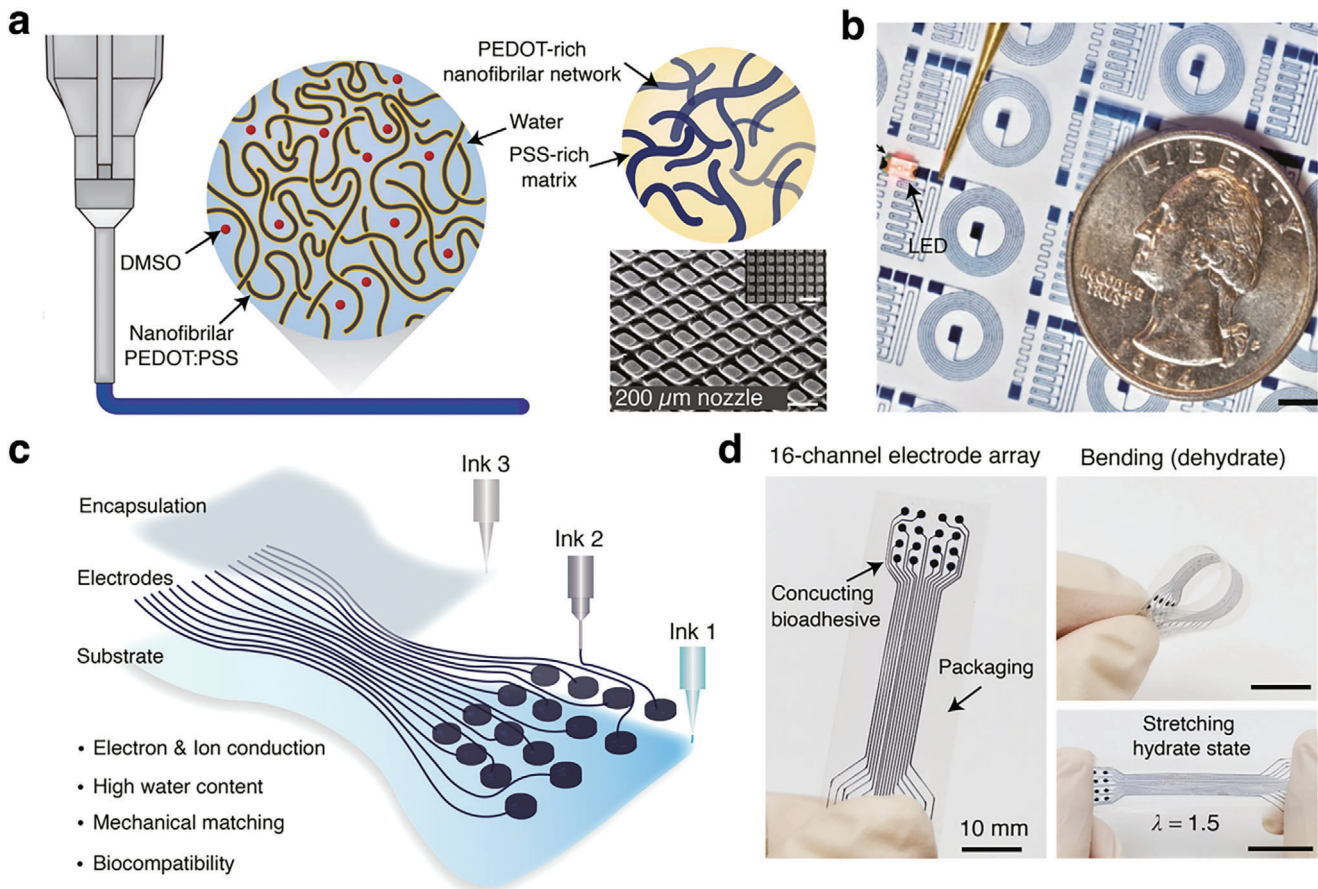
Figure 5. Laser-assisted patterned CHs. a) Schematic illustration of the laser-induced phase separation of CHs. b) Images of PEDOT microelectrode arrays. c) Images of a wet PEDOT circuit lighting a white LED. Reproduced under the terms of the CC-BY.[64] Copyright 2022, The authors, published by AAAS.

hydrogel, laser-induced phase separation has also been exploited for fabricating micropatterned PEDOT: PSS hydrogel electronics (**Figure 5**a).[66] Won et al. developed a highly conducting PEDOT hydrogel (conductivity of ≈670 S cm^{-1}) with a 6-μm spatial resolution through the laser-induced phase separation (Figure 5b,c).[64] PEDOT: PSS exhibits a phase-separated structure, with conducting PEDOT forming the core and insulating PSS constituting the shell. Notably, robust interconnections within the conducting yet hydrophobic PEDOT-rich domains ensure high electrical conductivity and aqueous stability. A continuous-wave laser, capable of delivering an intense electric field and photothermal energy within an ultrafast timescale, effectively drives the phase separation of PEDOT: PSS. By selectively scanning the target areas, the laser facilitates the formation of a patterned, PEDOT-rich conducting phase, significantly enhancing electron conductivity from 10 to 670 S cm^{-1}.[64] To enhance the interaction between PEDOT: PSS and the laser, plasmonic gold nanoparticles (AuNPs) were incorporated into the PEDOT: PSS matrix, effectively inducing the phase separation of PEDOT: PSS. Laser-assisted patterned hydrogel electronics offer the advantages of rapid processing and high efficiency in fabrication. However, the high processing temperature generated by high-energy lasers makes it challenging to apply this technique to hydrogel systems containing active substances, such as enzymes and bacteria, as the overheating can decrease their activity. Additionally, laser processing of low-reflectivity materials, such as black or transparent conducting hydrogels, can easily produce high-precision patterns.

3.5. Extrusion-Based Printing

Extrusion-based printing involves extruding a CHs precursor through a nozzle, which then solidifies on a substrate to form pre-designed patterns (Figure 3e). This technique offers the advantage of high spatial resolution and allows for the creation of intricate and complex patterns, with a reduced amount of CHs material used.[17b,67] Similar to screen printing, extrusion-based printing requires the ink to possess two essential rheological properties, shear thinning and rapid shear recovery, which are crucial for filament formation and maintaining the printed structures. However, commonly-used conducting polymer hydrogels precursors (i.e., PEDOT: PSS, <30 Pa s[17c]) are not viscous enough for the extrusion-based printing. The viscosity of PEDOT: PSS for extrusion-based printing can be finely controlled by introducing solvents to induce phase separation[17c] or incorporating long-chain polymers,[69] in order to modify its rheological properties. For instance, Yuk et al.[17c] developed a paste-like PEDOT: PSS ink by freeze-drying aqueous PEDOT: PSS suspension and re-dissolving the loosely structured PEDOT: PSS powders in a binary solvent mixture (water: DMSO = 85:15 v/v). The nanofibrillar PEDOT: PSS was intricately entangled within the solvent, causing the concentrated suspension to progressively transit from a liquid state to a thixotropic ink, which were suitable for extrusion-based printing (**Figure 6a,b**). Such kind of hydrogel inks exhibited distinct viscoelasticity, such as shear thinning (i.e., viscosity decreases from 10^2 to 10^{-1} Pa s up on the increase of shearing rate from 10^{-2} to 10^3 rad s^{-1}) and stress yielding. These unique rheological performances ensured good shape fidelity and precise control over the fabrication resolution (≈100 μm). Furthermore, functional hydrogel electronics could also be fabricated through multi-materials printing. Recently, Liu et al.[68] prepared a series of functional inks (i.e., conducting PEDOT: PSS inks, bioadhesion and encapsulation inks) to print implantable hydrogel bioelectronics through a multi-material DIW 3D printing (Figure 6c). The bioadhesive layer was mainly consisted of poly (acrylic acid-co-acrylic acid-N-hydroxysuccinimide ester) (PAA-NHS) and PVA, while the chemical crosslinker glutaraldehyde (GA) enabled the robust and reliable interfaci among functional layers. Extrusion-based printing is not only one of the most convenient methods for fabricating hydrogel electronics with

**ADVANCED
SCIENCE NEWS**

www.advancedsciencenews.com

**ADVANCED
FUNCTIONAL
MATERIALS**

www.afm-journal.de

Figure 6. Micropatterned CHs fabricated from extrusion-based printing. a) Schematic illustration of extrusion-based printing. b) Images of illumination of an LED on the 3D-printed conducting circuit. a,b) Reproduced under the terms of the CC-BY.[17c] Copyright 2020, The authors, published by Springer Nature. c) Schematic illustration of hydrogel bioelectronics through the extrusion-based multi-material 3D printing technology. d) Images of the 3D-printed all-hydrogel bioelectronics with 16 independent channels. c,d) reproduced with permission.[68] Copyright 2023, Wiley.

structural complexity but also allow for fabricating functional hydrogel electronics through multi-material printing. However, the shear thinning properties required in extruded inks impose high demands on viscosity, limiting the range of materials that can be used for hydrogel electronics processing.
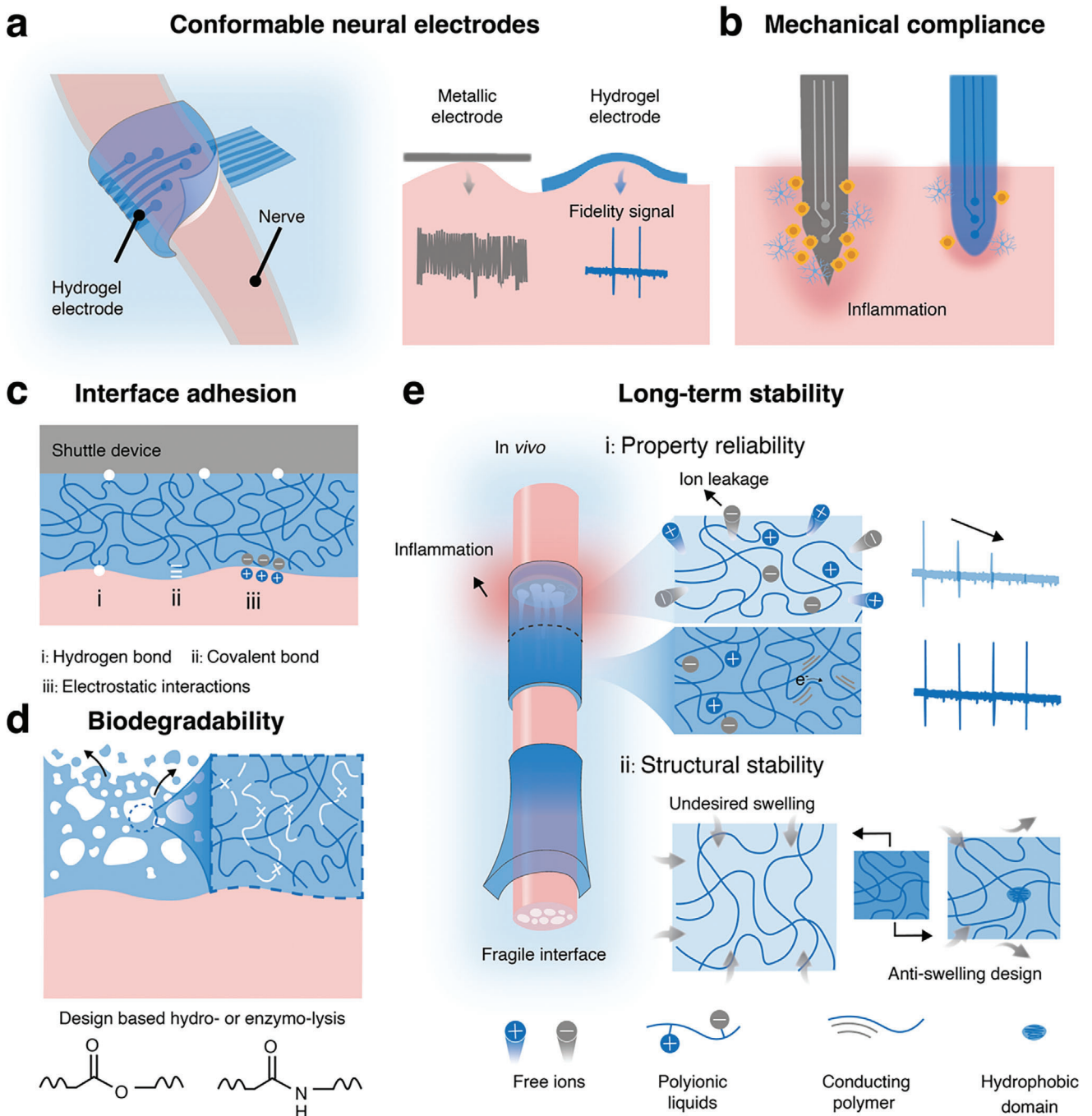
4. Key Requirements for CHs-Based Neural Bioelectronics

Depending on the specific implantable applications of neural bioelectronics, hydrogel electronics must meet additional requirements beyond conductivity and flexibility. This section will discuss the key requirements for hydrogel-based neural bioelectronics, including mechanical compliance with organs, adhesion to targeted tissues for real-time and accurate signal sensing, complete biodegradability over the operational lifespan, and long-term electrical and chemical stability.

4.1. Mechanical Compliance

Conventional neural bioelectronics (e.g., silicon, gold, platinum, and titanium nitride) exhibit a high Young's modulus

($E > 1$ GPa), which are several orders of magnitude higher than that of neural tissues ($E - 10$ kPa).[70] These biomechanical disparities not only prevent the establishment of mechanically compliant biointerfacing, but also lead to biological tissue damage and chronic immune responses. Due to their close similarity to biological tissues, CHs, with unique tissue-like mechanics (typically 1 to 100 kPa) and superior conductivity and biocompatibility, are promising for neural biointerfacing (**Figure 7a,b**).[71] For instance, Luo et al.[47] demonstrated that a PEDOT: PSS/PEGDA hydrogel electrodes ($E = 7.3$ kPa) could induce a mild inflammation during neural implantation, compared to the gold electrodes ($E = 77.2$ GPa). Upon 14-day implantation, the inflammatory infiltrated area was 70 μm for the PEDOT: PSS/PEGDA hydrogel electrodes, while 300 μm for gold electrodes. Additionally, in light of the electrochemical mismatch, high interface impedance between the neural tissues and metallic electrodes could also compromise the signal qualities.[49] The PEDOT: PSS/PEGDA hydrogel electrodes exhibited a lower impedance (≈ 160 Ω at 10^3 Hz) than that of platinum electrodes ($\approx 10^5$ Ω at 10^3 Hz). Under the same stimulation voltage of 1 V, the evoked peak-peak compound action potential (CAP) reached 8 mV for hydrogel electrodes, while only 4 mV of gold electrodes.

**ADVANCED
SCIENCE NEWS**

www.advancedsciencenews.com

**ADVANCED
FUNCTIONAL
MATERIALS**

www.afm-journal.de

Figure 7. Key requirements for implantable CHs-based neural bioelectronics. a) Schematic illustration of implantable neural bioelectronics. b) Schematic illustration of long-term implantation of mechanically-compliant neural electrodes with mitigated tissue damage and inflammatory response. c) Schematic illustration of the nerve-hydrogel biointerface. The hydrogel electronics are imparted with adhesion capability through interfacial formation of hydrogen bond, electrostatic interactions and/or chemical anchorage, in order to increase the interfacial robustness. d) Schematic illustration of the biodegradation of hydrogel electronics within the biological systems, without the need for removal through secondary surgery. e) Schematic illustration of long-term stability of hydrogel bioelectronics within biological systems. Hydrogel electronics are designed with reliable conductivity and swelling resistance, in sharp contrast to traditional metallic electronics which are prone to corrosion and fragment.

**ADVANCED
SCIENCE NEWS**

www.advancedsciencenews.com

**ADVANCED
FUNCTIONAL
MATERIALS**

www.afm-journal.de

4.2. Interfacial Adhesion

The reliable function of neural bioelectronics requires conformal and robust interfacial integration with the biological neural tissues.[72] Current interfacing are typically constructed using mechanical anchorage, accompanied with non-conformal contact, unstable attachment, tissue injury, and/or scar formation. To achieve mechanically conformable interface with dynamic wet tissues, hydrogel electronics are engineered with bioadhesion properties through molecular functionalization (e.g., hydrogen bonds, chemical anchorage and/or electrostatic interactions) to create the seamless biointerfacing (Figure 7c). Generally, the reliable neural biointerfacing is dominated by two interfaces, the hydrogel electrodes-neural tissue interface and the hydrogel electrodes-shuttle devices interface.[73] For the hydrogel electrodes-neural tissue interfacing, a dry crosslinking mechanism could be readily applied, by harnessing the synergistic contribution from both amide bond formation (NHS moieties within hydrogel part and amine moieties within the biological tissue part) and interfacial hydrogen bonds/electrostatic interactions.[74] With high interfacial toughness (i.e., 400–1000 J m^{-2}), such hydrogel electrodes could firmly adhere onto the surface of a periodically beating heart, enabling the real-time monitoring of cardiac rhythm without remarkable baseline shift or high-amplitude noise.[75] For the hydrogel electrodes/shuttle device (e.g., metallic or silicon microcircuits) interface, the shuttle device surface can be functionalized with acrylate groups, enabling the anchorage of polymer chains of the hydrogel networks. Together with the energy dissipation within the bulk hydrogel networks, interfacial toughness could reach ≈1500 J m^{-2}.[76] Furthermore, controllable tissue-electronics adhesion is crucial for the development of bioelectronic interfaces.[77] Although strong adhesion is beneficial for device performance, it can potentially cause discomfort or secondary injury during the detaching process. On-demand switchable hydrogel adhesions could be achieved by functionalizing the hydrogel networks with cleavable cross-links.[40d]
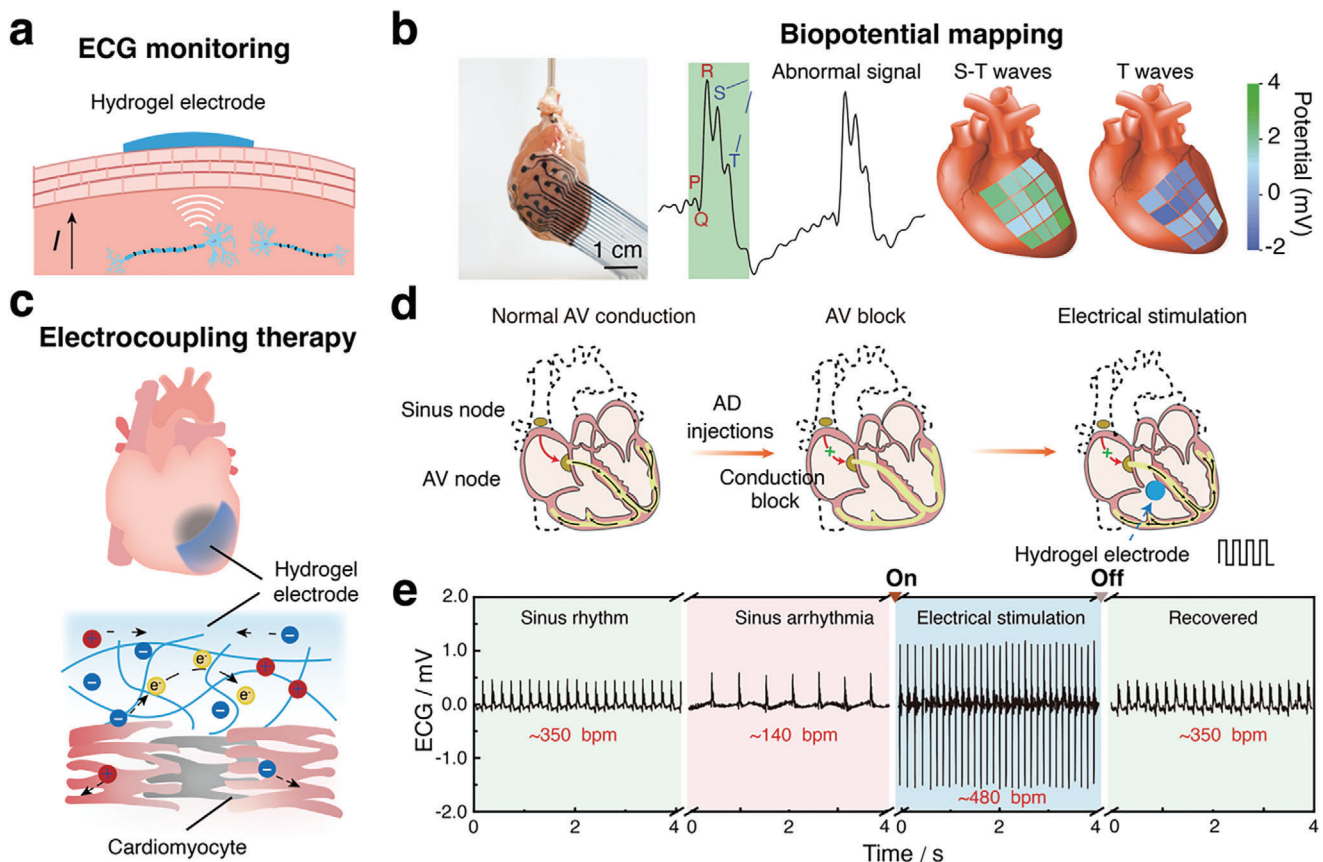
4.3. Biodegradability

Conventional neural devices need to be surgically removed once their therapeutic function is completed. However, the need for secondary removal surgery not only increases financial costs but also poses significant risks, including infection, tissue damage, and immune-mediated inflammation.[78] To mitigate these side effects, biodegradable or bioresorbable hydrogels have been employed in the construction of implanted neural devices (Figure 7d). Generally, hydrogels incorporating chemical bonds like ester, amide, and anhydride are susceptible to hydrolysis or enzymatic degradation.[17d,79] These hydrogel networks gradually destruct and dissolve within the biofluids, ultimately yielding bioabsorbables. For instance, polymer hydrogels made of natural polymers, e.g. chitosan, gelatin, alginate and hyaluronic acid, could readily degrade into small molecules and be excreted from the biological systems.[79b] However, natural polymer hydrogels with a high molecular weight (≈50 000 to 1 000 000 Da) are brittle due to hydrogen bonds among molecular chains, resulting in a degradation time of over months,[80] Synthetic hydrogels with

controlled molecular weight (≈from 1000 to 10 000 Da), such as polyethylene glycol (PEG), polyglycolic acid (PGA), and poly (lactic-co-glycolic acid) (PLGA), could be degraded within desired periods ranging from several hours to days.[81] To fulfil the requirements in specific application scenarios, the degradation rate of hydrogel devices can be precisely adjusted by modifying factors such as crosslinking density, thickness, and crystallinity of a degradable hydrogel electronics. The matrix of CHs can be designed for degradation through molecular weight control. However, conducting fillers such as metallic particles and carbon materials cannot be completely degraded in bioabsorbable products. However, nanoscale particles could be eventually metabolized and eliminated through metabolization process.[18d,82] Furthermore, biodegradable hydrogel electronics can also be utilized as a sacrificial material combined with therapeutic molecules, for the on-demand drug release and regeneration of the neural tissues.

4.4. Long-Term Stability

Long-term stability is a critical consideration for neural electronics used in dynamic organs with periodic motions (e.g., hearts, stomachs and lungs), and it is also determined by factors such as mechanical compliance, interface adhesion, and inherent chemical stability.[83] Apart from the aforementioned requirements, the chemical stability of hydrogel electronics will be thoroughly discussed in this section. As shown in Figure 7e, unlike traditional metallic electronics that are susceptible to oxidation or corrosion, hydrogel matrix remains relatively stable during long-term implantation due to their inert, crosslinked network structure, which is not sensitive to the biological fluids.[17e,68,84] For CHs, much effort should be focused on maintaining both property reliability and structural stability. Regarding property reliability, ensuring stable electrical conduction during long-term implantation remains a significant challenge. For instance, the ionic CHs electronics, such as hydrogels doped with NaCl or ionic liquids (as mentioned in Section 2), potential ion leakage into the surrounding biological fluid leads to a gradual decrease in the ionic conductivity of the hydrogel electronics. Moreover, the excessive number of ions disrupt the biological salt metabolism, posing severe biocompatibility risks. To address the ion leakage issue, ionic monomers can replace free ions in the doping process, incorporating them into the hydrogel polymer chain where they are covalently bonded, thus preventing significant ion leakage. The ionic monomers, such as 2-(Methacryloyloxy) ethyl dimethyl-(3-sulfopropyl) ammonium hydroxide (DMAPS) and 1-ethyl-3-methylimidazolium trifluoroacetate (TFA), can be utilized to fabricate hydrogel electronics with minimal ion leakage.[85] The structural stability of CHs aims to maintain control over the hydrogel's dimensions. For all hydrogel matrices, undesirable swelling during the long-term implantation inevitably leads to a loss of functional stability (i.e., mechanical, adhesive, and conducting properties). To date, various design principles have validated the engineering of hydrogels with anti-swelling performances, by introducing strong electrostatic interactions, hydrophobic phase segregation, or increasing the crosslink density of hydrogel to avoid uncontrolled swelling.[86] For example, Gong et al.[87] used sodium styrene sulfonate (anion) and N, N-dimethylaminoethyl acrylate (cation) to form a

**ADVANCED
SCIENCE NEWS**

www.advancedsciencenews.com

**ADVANCED
FUNCTIONAL
MATERIALS**

www.afm-journal.de

Figure 8. CHs-based bioelectronics for cardiac interfacing. a) Schematic illustration of mechanism for electrophysiological recording. b) High-precision monitoring of abnormal ECG signals for acute myocardial infarction using 3D-printed CHs. Abnormal S and T peak signals are recorded via a 16-channel CHs electrode array. Reproduced with permission.[68] Copyright 2024, Wiley. c) The chronological adhesive hydrogel patch (CAHP) for synergistic cardiac mechanophysiological monitoring and electrocoupling therapy. d) In vivo treatment of atrioventricular (AV) block and ECG monitoring using conducting polymer hydrogel-coated bioelectrode. e) The autonomous rhythm is restored by electrical stimulation delivered through conducting polymer hydrogel-coated bioelectrode. c-e Reproduced with permission.[28] Copyright 2023, Wiley.

polyampholyte hydrogel, which creates a dual-continuous phase network through strong electrostatic interactions, thereby achieving anti-swelling properties. Additionally, introducing hydrophobic groups into the hydrogel can also prevent swelling. Ran et al.[88] synthesized a gel using acrylic acid and 2-ethylhexyl acrylate (HEA) in dimethyl sulfoxide (DMSO). During solvent exchange (with water replacing DMSO), PHEA induced microphase separation due to its poor affinity with water. This hydrogel exhibited excellent anti-swelling performance even after 15 days of immersion in an acidic environment (pH = 3.0). Furthermore, encapsulation of hydrogel electronics with a hydrophobic layer (e.g., polyurethane or polydimethylsiloxane) represents another strategy to impart the hydrogel electronics with superior resistance to excessive swelling during the long-term implantation.[89]

5. Application Scenarios of CHs-Based Bioelectronics for Neural Biointerfacing

Hydrogel electronics for neural biointerfacing can significantly enhance the functions of implantable bioelectronic devices, simulate neuronal behavior, and serve as ideal materials for next-generation neural biointerfacing technology in a wide range

of fields, including cardiac interfacing, neural tissue repairing, brain-machine interfaces, brain-like neural communication, and electromyographic monitoring.

5.1. Cardiac Interfacing

The heart acts as the body's engine. Each heartbeat begins with an electrical impulse generated by the sinoatrial (SA) node, which then transmits and stimulates the contraction of the atrial muscles, pumping blood stored in the atria into the ventricles and subsequently into the systemic circulation.[90] However, patients with cardiovascular disease may experience functional impairments such as delayed or excessively fast electrical signals, as well as uncoordinated or asynchronous cardiac contractions.[91] Therefore, cardiac interfacing for monitoring electrical or mechanical signals is essential for the diagnosis and treatment of cardiovascular diseases (**Figure 8a**). However, establishing effective long-term interfacings with the curved surface of a heart that beats dynamically presents substantial challenges, particularly in case of high-quality electrophysiological monitoring, electrical stimulation, and mechanical assistance.[92] Conventional

**ADVANCED
SCIENCE NEWS**

www.advancedsciencenews.com

**ADVANCED
FUNCTIONAL
MATERIALS**

www.afm-journal.de

implantable devices for electrotherapy and mechanical circulatory support provide substantial clinical benefits. However, the rigid electrodes inevitably raise the risk of device dislodgment, infection, tissue damage, and scar tissue formation.[93] CHs-based electronics, with key properties akin to cardiac tissue, such as a modulus of 570 kPa, stress of 240 kPa at 30% strain, fracture strain of 120%, and electrical conductivity superior to that of cardiac tissue (9 S m^{-1}), are widely employed in multi-channel cardiac interfacings (Figure 8b).[68,94] Furthermore, ionic hydrogels can not only precisely locate the site of myocardial infarction through multi-channel data (64-channel array), but also monitor strain information during heartbeats, presenting an innovative solution for the real-time tracking of dynamic changes in cardiac diseases.[95] Additionally, conducting polymer hydrogels can enhance the electrophysiological activity in the myocardial infarction region through electromechanical coupling, enabling therapeutic intervention for the cardiac dysfunction.[96]

Despite these advancements, the issues of device-organ adhesion and long-term biocompatibility during implantation remain important concerns. Hydrogel-based bioelectronic patches demonstrate rapid tissue adhesion (less than 0.5 s), stable interfacial compliance (7.2 kPa against shear stress, 660% stretching), and long-term biocompatibility (4 weeks), while facilitating electrophysiological monitoring and electrical stimulation (2.5 V).[97] Moreover, a cardiac mesh structure designed as a soft robotic sleeve can greatly enhanced the cardiac ejection function, while incorporating hydrogel as a protective interfacing layer effectively improved its biocompatibility (up to 2 weeks).[98] Similarly, using CHs as coatings on conventional metallic electrodes for cardiac pacing can enhance the electric stimulation efficacy and reduce the pacing threshold voltage.[28] The precise localization of cardiac lesions is crucial for the diagnosis and treatment of cardiovascular diseases (Figure 8c–e). Future research should focus on developing more defined sensing interfacing, such as high-density, stretchable electrode arrays (less than 100 μm, similar to a single cardiomyocyte), for real-time, stable, cellular-level-resolution electrophysiological mapping.[99]

5.2. Neural Tissue Repairing
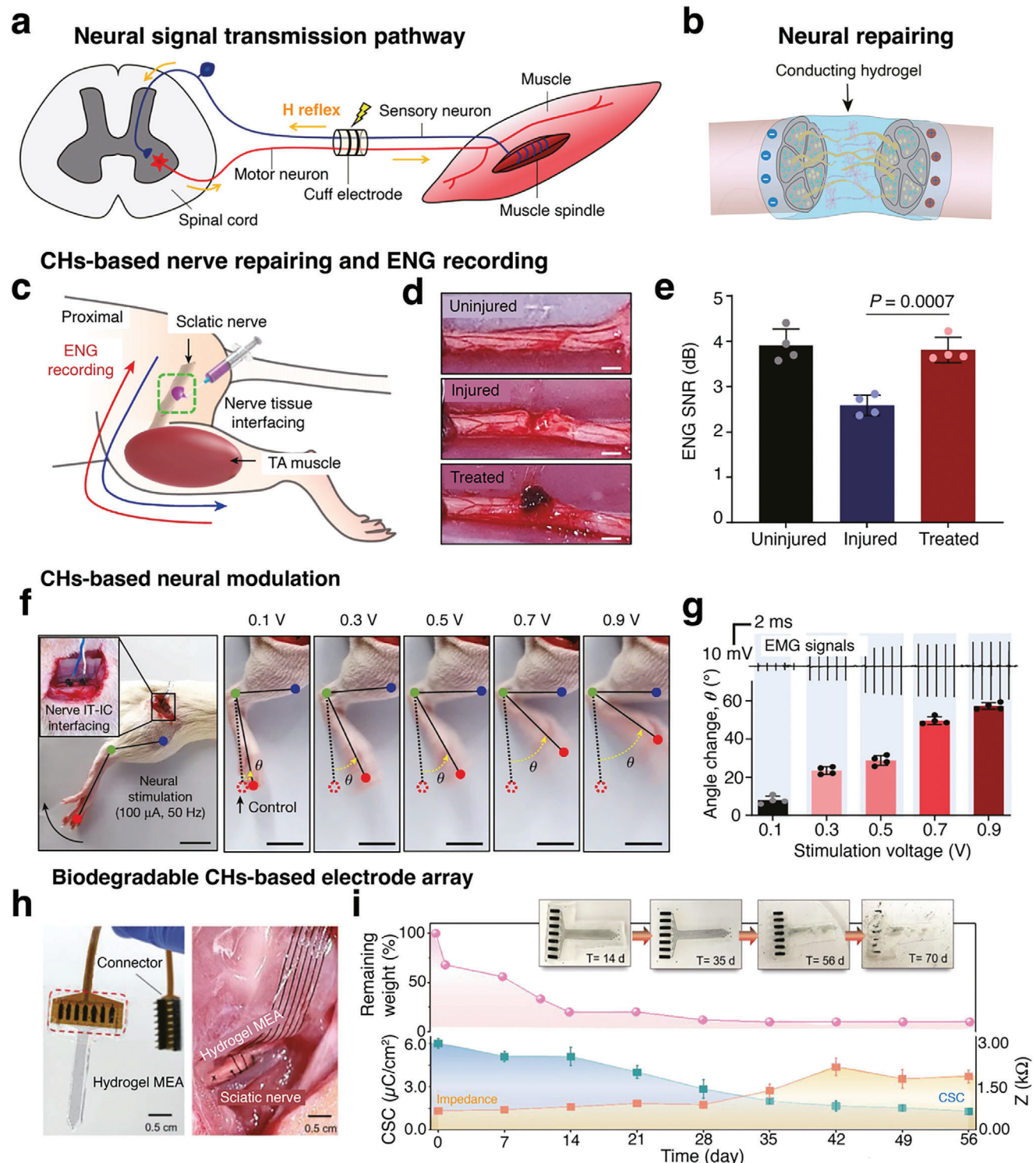
The transmission of information between the brain and various parts of the body is mediated by multiple neural systems. Damage to the neural system, such as spinal cord injury (SCI), peripheral nerve injury (PNI), and cranial nerve injury, can result in partial loss of movement or other functions.[102] The injured central neural system contains a high concentration of inhibitory molecules, including myelin-associated proteins[103] and proteoglycans at glial scars,[104] which hinder the nerve regeneration. Autologous nerve transplantation, traditionally regarded as the gold standard in clinical treatment, faces significant challenges, including complex surgical procedures, limited donor sites, potential loss of nerve function, and scar formation. Extensive research has been devoted to developing synthetic alternatives, such as nerve guidance conduits (NGCs), which provide temporary mechanical support and a favorable microenvironment for nerve regeneration. Notably, since signal transmission in neural pathways depends on electrical signals, re-establishing electrical pathways is crucial for effective nerve repair (**Figure 9**a). The

CHs can be used to construct electrical signal pathways at the injured neural interfacing, thereby restoring nerve signal transmission function (Figure 9b). It has been demonstrated that NGCs made from conducting polymers, such as PPy, can promote axonal growth at sites of sciatic nerve tissues injury.[105] However, as most NGCs are commonly in the form of patches, their applicability in narrow, complex, and small biological interfacing is limited. To address this issue, an injectable CHs can be used to treat injured sciatic nerves, reconstruct electrical pathways, and successfully record ENG signals similar to those of uninjured sciatic nerves (Figure 9c–e).[100]

In addition to utilizing CHs-based NGCs for nerve tissue repairing, CHs demonstrate great potential in neural bioelectronics, particularly in applications of electrical stimulation (ES). Injectable tissue-interfacing prostheses hydrogels enable efficient regulation of electrical signal transmission between nerves and muscles, thus inducing ankle joint angle changes in mice under different stimulation voltages (100 μA, 50 Hz), with angles significantly increasing as the voltage rises (Figure 9f). Simultaneously, EMG signal recordings show progressively enhanced amplitudes with increasing voltages, further confirming their superior performance in electrical stimulation (Figure 9g). In addition, the CHs-based neural repairing system can degrade in biological fluids, reducing the need for invasive retrieval procedures. In vitro experiments in PBS showed that the MEA lost over 45% of its weight within 7 days but retained sufficient structural integrity for electrochemical measurements. After 28 days of degradation, the device still maintained the CSC of 1.99 μC cm^{-2} and an impedance of 1.6 ± 0.8 kΩ, demonstrating its ability to sustain functionality during gradual degradation (Figure 9h,i).[101]
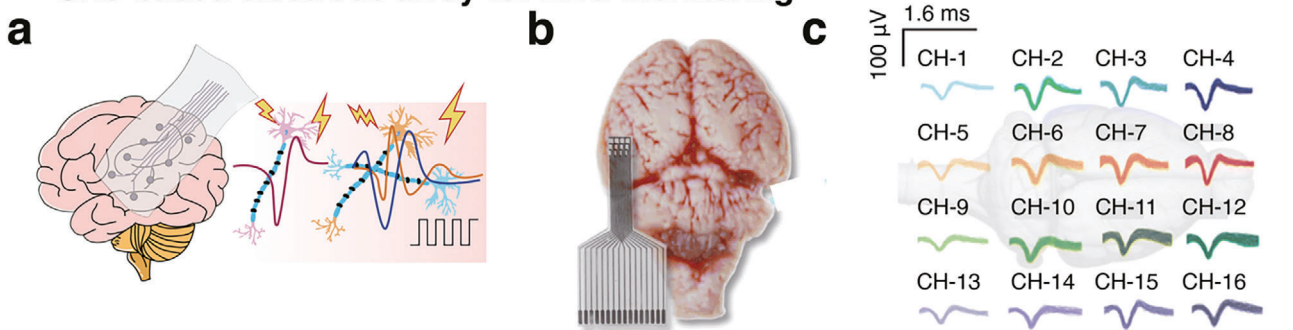
5.3. Brain-Machine Interfaces

The brain is the most vital organ in the body, yet its accessibility remains limited, making the continuous and accurate monitoring of brain activities, as well as feedback-based therapy, a long-lasting challenge. Implantable brain-machine interfaces can accurately detect brain activity and actively deliver stimulation, offering significant potential in the diagnosis and treatment of brain diseases (**Figure 10**). In terms of monitoring, key indicators includ ing electroencephalography (e.g., electroencephalogram, electrocorticogram or stereoelectroencephalography), intracranial pressure detection, pH levels, and intracranial temperature, are clinically recorded. Conventional probes and arrays used for acquiring electroencephalography signals often trigger significant foreign-body responses, severely compromising their long-term reliability and functionality. Soft neural implants, such as e-dura,[108] demonstrate long-term biointegration for over 6 weeks and possess a Young's modulus of 1 MPa. In contrast, CHs-based bioelectrodes typically exhibit Young's modulus ranging from a few hundred Pa to 1 MPa, making them more compatible with neural tissues. The neural interfacing formed through CHs-based bioelectrodes can record real-time brain activities for up to six months,[109] which aids in reducing tissues damage, and foreign-body responses. It is also capable of recording the subtle neural activity of single or multiple neurons (Figure 10b).[106] In intracranial pressure monitoring, a biodegradable pressure sensor could effectively reduce the damage and infection risks
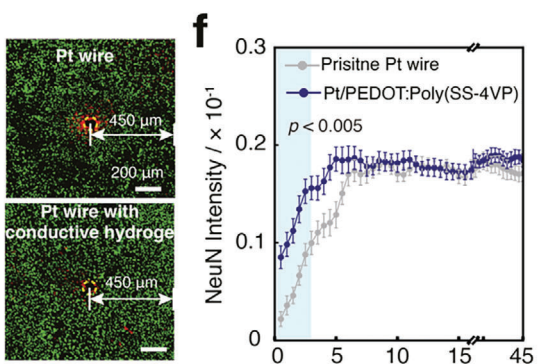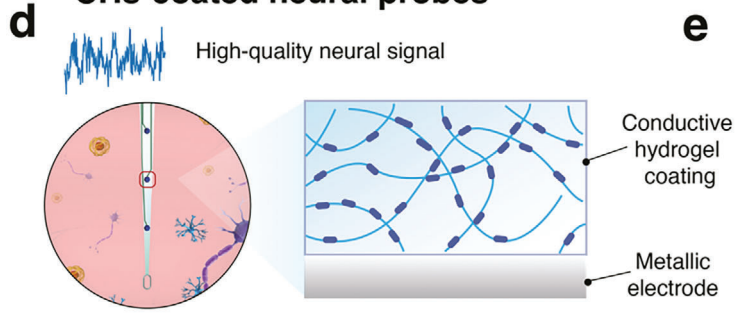
Figure 9. CHs-based bioelectronics for neural tissue repairing. a) Bidirectional sensory and motor signalling in the neuromuscular system. b) CHs for repairing nerve electroneurogram. c) CHs-based nerve repairing and electroneurography (ENG) recording. d) The CHs are implanted into the injured sciatic nerve to establish a conducting pathway. e) The treated injured sciatic nerve exhibits ENG signals similar to those of the uninjured sciatic nerves. f,g) CHs-based neural modulation. Neural stimulation is achieved using CHs through neural interfacing, with photographs showing ankle movements through electrical stimulation and the corresponding electromyography (EMG) signals. c-g Reproduced with permission.[100] Copyright 2023, Springer Nature. h,i) The biodegradable microelectrode array (MEA) composed of bioactive, biodegradable, and adhesive silk/gelatin hydrogel is used for electrical stimulation of the sciatic nerve and degrades nearly completely within 70 days in PBS at 37 °C. h,i) Reproduced with permission.[101] Copyright 2023, Wiley.

**ADVANCED
SCIENCE NEWS**

www.advancedsciencenews.com

**ADVANCED
FUNCTIONAL
MATERIALS**

www.afm-journal.de
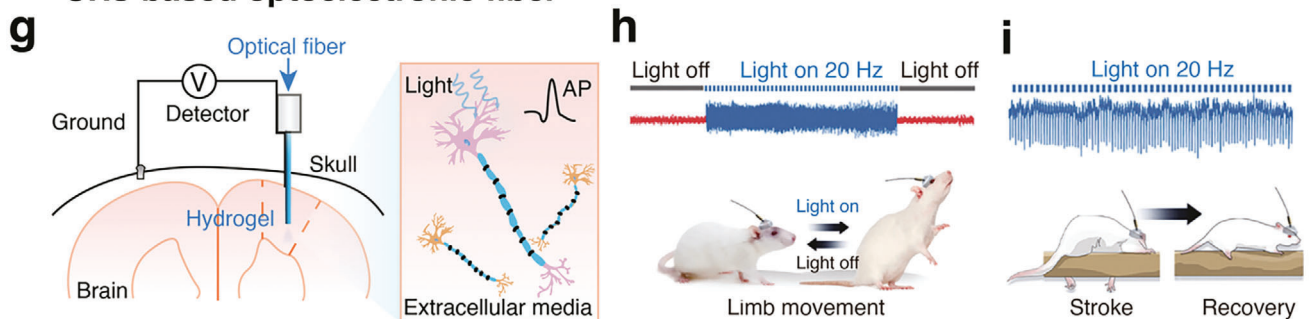
CHs-based electrode array for EEG monitoring
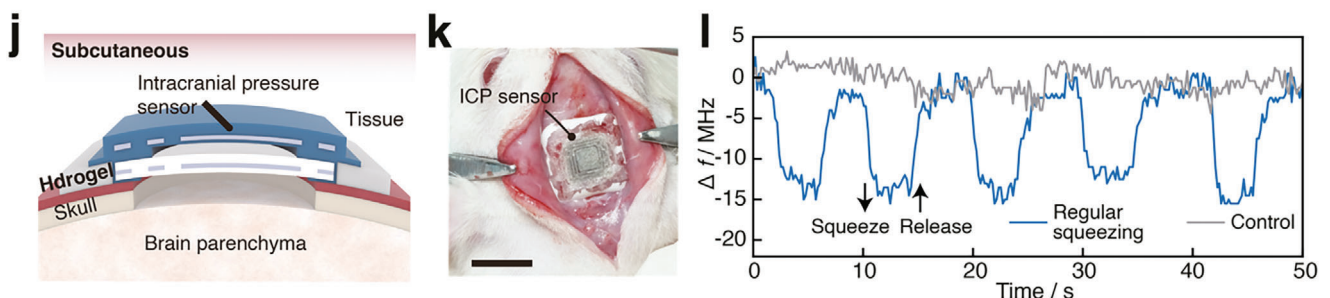
CHs-coated neural probes

CHs-based optoelectronic fiber

Implantable bioelectronics for intracranial pressure monitoring

Figure 10. CHs-based bioelectronics for brain-machine interface. a) Schematic illustration of CHs electrode array for electroencephalogram (EEG) monitoring or electrical stimulations. b,c) All-hydrogel 16-channel electrode arrays for in vivo monitoring of action potentials. Reproduced with permission.[106] Copyright 2024, Royal Society of Chemistry. d) Schematic illustration of metallic neural probes coated with CHs. e,f) The coating of CPHs could effectively endow the electrodes with superior biocompatibility, electrical and mechanical properties. d–f) Reproduced with permission.[8c] Copyright 2022, Wiley. g–i) CHs-based optoelectronic fibers for optogenetic neuromodulation. Implantable neural probes with the topological hydrogel could effectively reduce the infarct regions of the brain tissue and promote locomotor function recovery by optogenetic neuromodulation. Reproduced with permission.[107] Copyright 2023, Wiley. j–l) Implantable electrodes for intracranial pressure monitoring. Biodegradable pressure sensor by utilizing a hydrogel-based bio-adhesion strategy to achieve wireless and real-time monitor the intracranial pressure.[40c] Copyright 2024, Wiley.

**ADVANCED
SCIENCE NEWS**

www.advancedsciencenews.com

**ADVANCED
FUNCTIONAL
MATERIALS**

www.afm-journal.de

associated with secondary surgery; however, it suffers from limited interfacing stability.[110] By utilizing a hydrogel-based bioadhesion strategy, Liu et al. could apply a biodegradable pressure sensor to wireless and real-time monitor the change in intracranial pressure with a sensitivity of 1 MHz mmHg^{-1} (Figure 10j–l).[40c]

Regarding active electrical or optical stimulation, traditional methods that rely on magnetic coupling for radiofrequency power transmission to achieve nerve electrical stimulation are relatively complex.[111] While implanted optical fiber materials can regulate brain neural activity through optical stimulation, the bending stress on optical fiber probes is considerable, ranging from 14 to 28 MPa, which can potentially damage brain tissues.[112] Hydrogel-based hybrid probe demonstrates a variable Young's modulus ranging from 16.5 kPa to 50 MPa, along with improved biocompatibility (exhibiting stable performance at lateral and longitudinal amplitudes of 100 μm). This probe enabled optogenetic stimulation and electrophysiological monitoring within the targeted stimulation area, thereby facilitating a control-feedback closed-loop for neural regulation (Figure 10g).[109] It can effectively reduce the infarct region of brain tissues, promote locomotor function recovery by optogenetic neuromodulation, and realize the treatment of brain diseases (Figure 10h,i).[107] Recent studies have also demonstrated that the CHs coating could effectively endow the traditional electrode with superior biocompatibility, electrical and mechanical properties. Fluorescence imaging after 8-week implantation revealed reduced accumulation of reactive astrocytes around metal electrodes with CHs coatings compared to uncoated electrodes, along with higher neuronal nucleus intensities (Figure 10e,f).[8c] At the same time, CHs-based electrodes, with high charge capacity (i.e, 1.3 mF), enhanced ion migration (2.59 cm^2 V^{-1} s^{-1}) and a stable mechanical interfaceing, could also be utilized to provide efficient electrical stimulation when placed on the skull.[113] In the future, soft probes based on hydrogels could enable stable electrophysiological recording and high-charge electrical stimulation, offering a potential therapeutic strategy for refractory epilepsy, brain tumors, and other neurological diseases.

5.4. Brian-Like Neural Communication
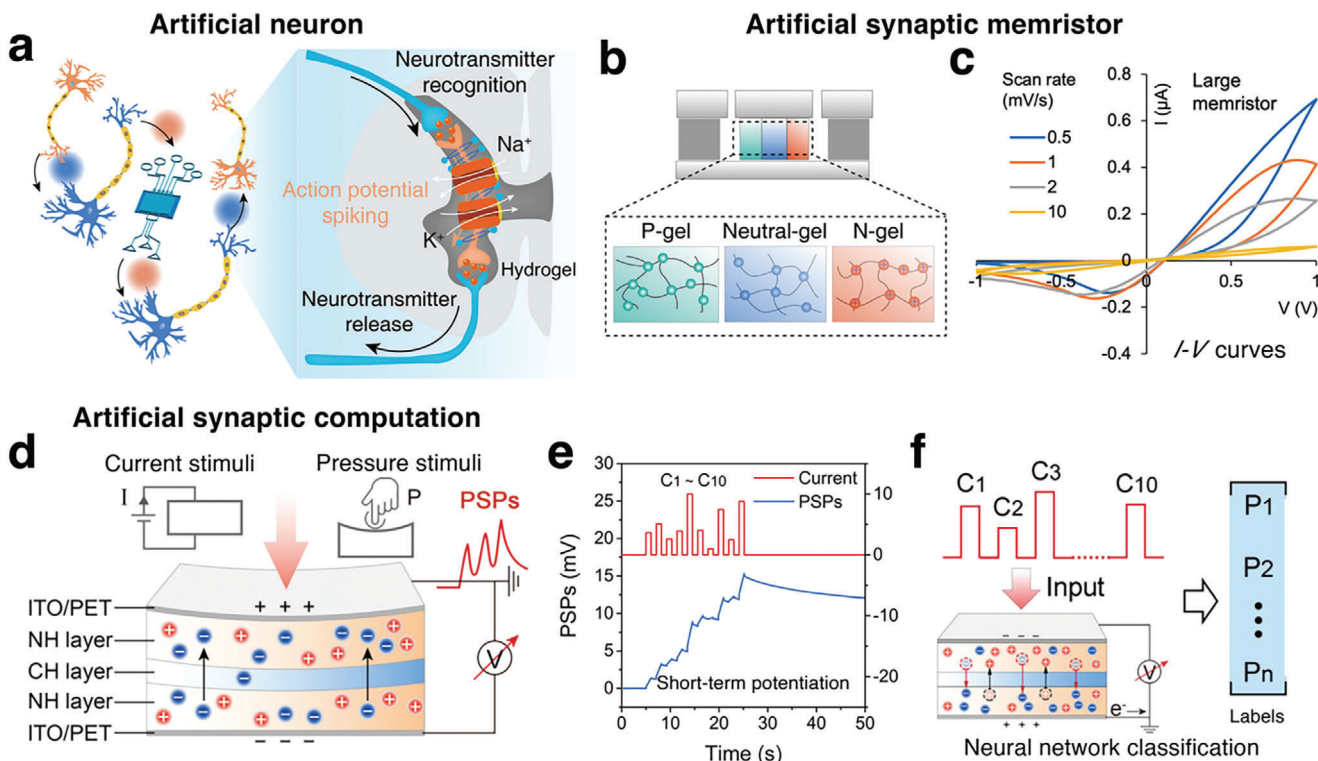
The human brain can perform parallel computing, perception, and memory effects with very low energy consumption. The brain functions are sustained by $\approx 10^{11}$ neurons, which are interconnected through synapses that enable the transmission of electrical and chemical signals.[116] Among these, advanced cognitive functions like memory and emotion are encoded or transmitted by chemical molecules, including the neurotransmitter dopamine.[117] The main functions of synapses include neurotransmitter recognition, synaptic plasticity, action potential firing, and neurotransmitter release.[118] Since hydrogels could be engineered with excellent ionic conductivity, biocompatibility, and stimulus response characteristics, they are one of the most promising materials for realizing artificial synaptic functions (**Figure 11a**).[119]

Most recently, Chen et al.[7] reported an artificial neuron with chemical-mediated capabilities, including an electrochemical sensor module (it exhibits a linear range of 1 μM to 1.5 mM)

for detecting dopamine and a hydrogel thermal response module (within a temperature range of 37.5–43.5 °C) for releasing dopamine. Such artificial neuron possessed chemical communication capabilities, allowing it to replace interneurons or motor neurons for decision-making or motor feedback.[7] BMIs based on electrical signals cannot fully translate brain information, whereas this chemically mediated artificial neuron can interpret neuronal information more accurately and comprehensively, and it could be developed into an artificial sensory system with expanded functions in the future. Another application is to simulate the characteristics of high-throughput computing and low energy consumption (<20 W) of synapses. Specifically, synapses can adjust the strength and efficiency of signal transmission based on the type and intensity of input signals, similar to the "switch" mechanism in modern computing systems. Traditional transistors or memristors are made of metal materials, which makes miniaturization challenging and renders them non-biodegradable. Through bionic research, exploring artificial devices that precisely control ion transport will help promote the development of ultra-low energy consumption information technology in ion systems. The voltage-controllable ion channels have been prepared using carbon nanotubes, which exhibits an on/off ratio of 10^4 at operation gate voltage as low as 1 V.[120] However, they face challenges such as high fabrication complexity, limited ion selectivity, and fixed morphology. In contrast, hydrogel ion channels provide superior ion selectivity, simply fabrication, and tunable morphology, making them more versatile for a wide range of applications. Yossifon et al.[114] developed a three-layer conducting hydrogel with varying ion selectivity, which exhibits an ion concentration polarization effect (ICP), enabling prolonged memory time along with large memristive current-voltage (I–V) curves, thereby achieving performance comparable to memristors (Figure 11b,c). Meanwhile, Xiao et al.[115] leveraged the ionic potential relaxation effect in the sandwich-structured hydrogels, using ions as information carriers to enable memory effects and experiential learning capabilities, akin to the neural network-weighted computation and classification in artificial intelligence (Figure 11d–f). Voltage-controllable hydrogel ion channels offer distinct advantages, including low power consumption, flexibility, excellent biocompatibility, and enhanced ion selectivity. In the future, it can be used as a more accurate, intelligent, and efficient artificial intelligence sensing carrier.[121]

5.5. Electromyographic Monitoring

Skin serves as the primary interfacing through which the human body perceives the external world, while the underlying muscular tissues forms the foundation for human movement. Mechanoreceptors and tactile neurons beneath the skin alter their membrane potential in response to external stimuli, converting these stimuli into electrical pulses with varying frequencies, which are then transmitted to the brain's central nervous system for cognitive processing and decision-making.[126] Non-invasive and effective acquisition of multifunctional physiological signals through the skin has significant implications for daily health monitoring, clinical disease diagnosis and treatment, and sports rehabilitation. For instance, surface electromyography (sEMG) signals generated by muscle stretching or contraction during

**ADVANCED
SCIENCE NEWS**

www.advancedsciencenews.com

**ADVANCED
FUNCTIONAL
MATERIALS**

www.afm-journal.de

Figure 11. CHs-based bioelectronics for brain-like neural communication. a) Artificial neuron with chemical-mediated capabilities based on CHs could replace interneurons or motor neurons for decision-making or motor feedback. Reproduced with permission.[7] Copyright 2022, Springer Nature. b,c) Three-layer CHs with varying ion selectivity, which achieved prolonged memory time along with large memristive current-voltage ($I–V$) curves. Reproduced with permission.[114] Copyright 2024, American Chemical Society. d–f) Ionic potential relaxation effect in the sandwich-structured hydrogels, which achieved memory effects and experiential learning capabilities, and akin to neural network-weighted computations in artificial intelligence. Reproduced with permission.[115] Copyright 2024, American Chemical Society.
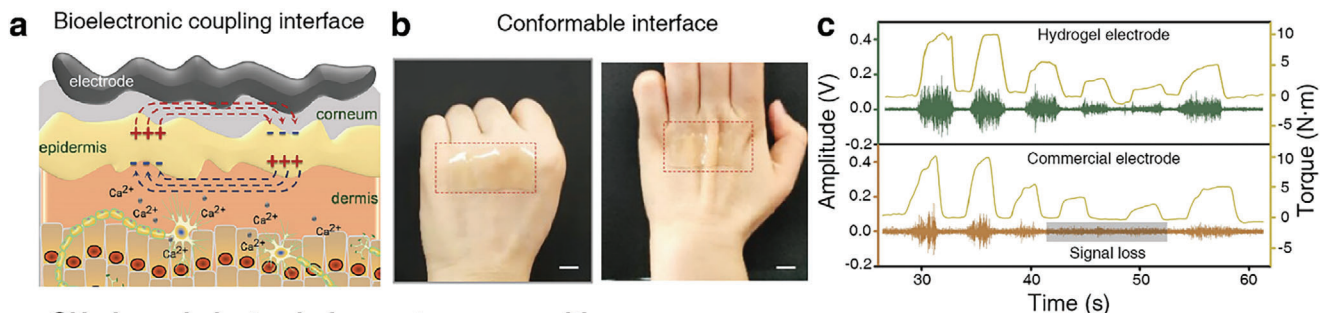
human movement, provide valuable insights into motor function and physiological status. In recent decades, the rapid advancement of wearable electromyography sensors has created an urgent need for soft and flexible sensing interfacings capable of establishing highly conformal contact with wrinkled, stretchable, and dynamically changing skin surfaces, thereby enhancing the collection and transmission of transdermal physiological signals.

However, the uneven, soft, and deformable nature of the skin, coupled with sweat production during physical activity, poses significant challenges for conventional rigid electrode materials. These materials fail to effectively capture sEMG signals, resulting in signal attenuation or loss of critical data, which may ultimately lead to misinterpretations or misdiagnoses. In contrast, CHs offer superior properties, including excellent adhesion, mechanical softness, and strong resistance to sweat interference (**Figure 12a,b**). Their ultra-low impedance ($\approx$50 kΩ), Young's modulus ($\approx$59 kPa) of skin-like, and superior signal-to-noise ratio ($\approx$32 dB) enable the stable and reliable acquisition of multimodal physiological data on skin surfaces (Figure 12c). Moreover, such interfacing can reduce signal crosstalk and resist interference from motion artifacts or skin deformation, enabling more accurate data acquisition. This capability is particularly valuable for the simultaneous monitoring of human movement and sEMG signals during exercise, facilitating the effective evaluation of an athlete's daily training and the development of scientifically informed training programs.
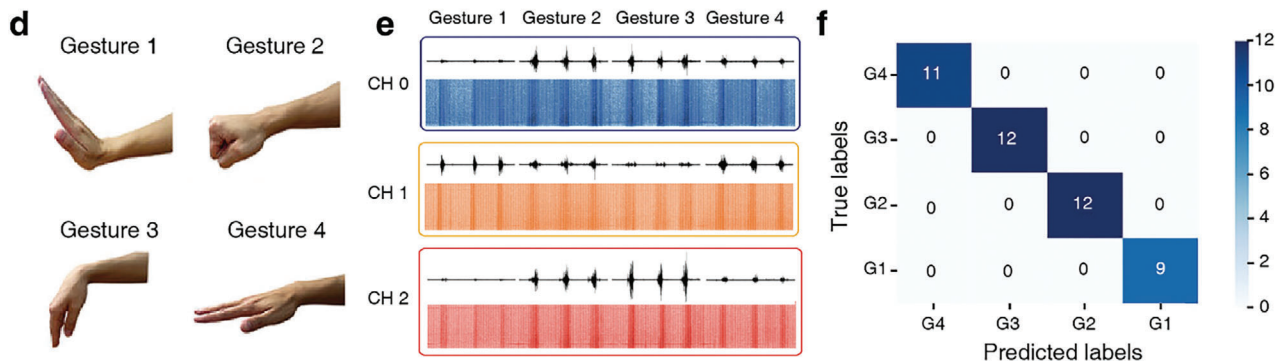
Li et al.[123] has developed CHs electrodes capable of capturing high-quality EMG signals. By combining these signals with advanced statistical methods like linear discriminant analysis (LDA) and machine learning algorithms such as Artificial Neural Networks (ANN), they effectively encoded and identified four unique gestures: wrist extension, fist clenching, wrist flexion, and finger spreading (Figure 12d). The time-frequency thermograms of the raw EMG signals and the four gestures are presented in Figure 12e, illustrating distinct energy distributions across the four channels for each gesture, with higher amplitudes corresponding to greater muscle output. The raw EMG signals were processed through filtering, noise reduction, and feature extraction. These extracted features were then utilized by the ANN for model training and data analysis. When employing the ANN, the classification and prediction accuracy for the validation set of gestures reached 100% (Figure 12f). Additionally, the validation R^2 value steadily converged toward 1 (0.98763) with increasing epochs, while the validation error decreased to 0.000599, demonstrating the robustness and precision of the model.[42,122,127]

Conversely, with the rapid development of intelligent prosthetics and humanoid robotics, accurately interpreting human behavioral intentions has become a critical aspect of human-computer interaction. CHs-based sensors offer distinct advantages by obviating the need for complex circuit boards or electrode structures, rendering them particularly well-suited as perceptual media for future human-machine interfaces.[128] These sensors
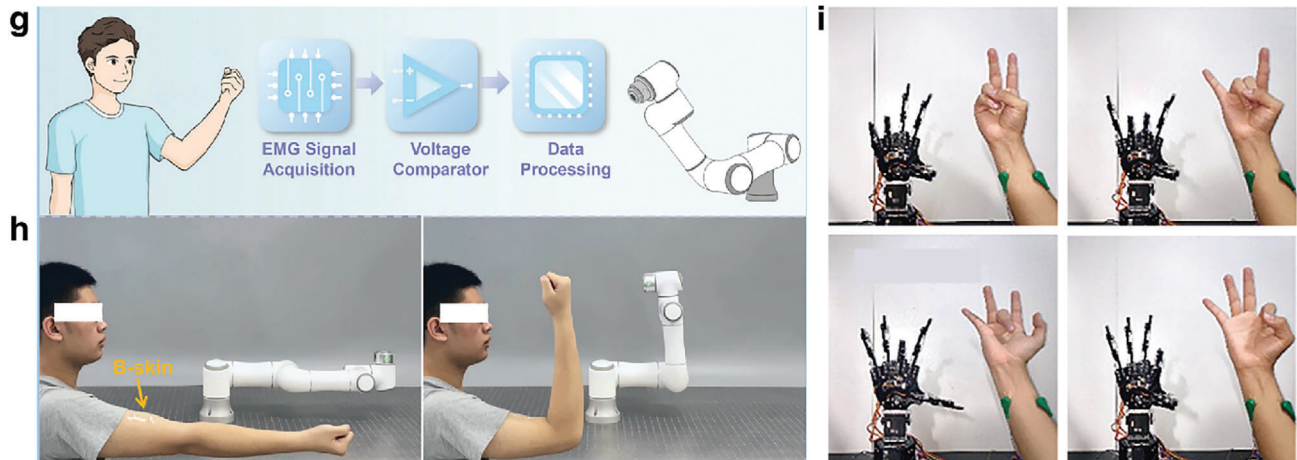
**ADVANCED
SCIENCE NEWS**

www.advancedsciencenews.com

**ADVANCED
FUNCTIONAL
MATERIALS**

www.afm-journal.de

Figure 12. CHs-based bioelectronics for electromyographic monitoring. a) Schematic illustration of CHs for electromyographic monitoring. b) Images of CHs with a conformable interfacing with skins. c) Compared to commercial electrodes, CHs electrodes offer a higher signal-to-noise ratio when recording electromyographic signals and can capture weaker signals without signal loss. a,c) Reproduced with permission.[122] Copyright 2022, American Chemical Society. b) Reproduced with permission.[42] Copyright 2022, Wiley. d–f) Multichannel analysis and gesture recognition using EMG signals recording from CHs by machine learning. Reproduced with permission.[123] Copyright 2024, Wiley. g,h) Synchronous robotic arm control system using straighten/bend EMG signals of the human arm collected by CHs electrodes. Reproduced with permission.[124] Copyright 2023, Wiley. i) Robotic hand with multiple fingers can be controlled by precise EMG signals from two or more CHs electrodes working together. Reproduced with permission.[125] Copyright 2021, Elsevier.

enable high-precision electrophysiological signal acquisition, making them invaluable for activity-based human control systems. For instance, the bioprotonic skin (B-skin) can capture EMG signals from the straightening and bending of a human arm, which can then be used to coordinate the movements of a robotic arm (Figure 12g). Leveraging this capability, an intelligent

robotic control system was designed by combining the artificial skin with the user's upper arm to capture EMG signals. During arm straightening or bending motions, the captured EMG signals are processed in real-time by a microcontroller, converting them into control commands that effectively direct the robotic arm to replicate these movements (Figure 12h). Furthermore, the

**ADVANCED
SCIENCE NEWS**

www.advancedsciencenews.com

**ADVANCED
FUNCTIONAL
MATERIALS**

www.afm-journal.de

precise EMG signals enable fine control of individual robotic fingers, including subtle twisting angles. When multiple hydrogel-based electrodes operate synergistically, they can generate precise control over multiple robotic fingers (Figure 12i).

6. Prospectives

CHs-based neural biointerfacing is poised to make a significant impact on the field of neural engineering, bridging gaps that conventional materials have struggled to overcome. Coupling with the ongoing advancements in CHs design principles, fabrication technologies, hydrogels electronics have the potential to revolutionize neural biointerfacing technology. Despite recent progress, there remain some critical issues and untapped opportunities in the development of hydrogel-based neural biointerfacing technologies, which provide plenty space for future material innovation and technical development. Herein, the critical issues and the potential directions for further development of CHs are discussed in the following aspects.

1) *Long-term reliability*: For implantable neural interfacing, the long-term reliability of CHs is critical for their practical application. Beyond the structural stability and performance reliability as discussed earlier, the functional reliability of CHs-based neural biointerfacing remains a challenge due to dynamic loading from neural activity during prolonged interaction in biological environments. Specifically, CHs are prone to fatigue fractures and functional failure under repeated mechanical loading cycles, necessitating enhanced fatigue resistance to maintain functional reliability. Inspired by natural structures like sciatic nerve, heart valves, muscles, and cartilage, significant advances have been made in engineering hydrogel materials with unprecedented fatigue-resistant performances.[129] Recent studies demonstrated that hydrogels can attain remarkable fatigue resistance through bioinspired hierarchical designs, including nanoscale minerals,[130] preferentially-aligned micro/nanostructures,[131] and fibrillar architectures.[132] These strategies enabled sophisticatedly-tailored microstructures for CHs- based electrodes, with greatly improved fatigue resistance, as validated by over millions cycle dynamic loading.[131,133] Thus, achieving long-term mechanical robustness in CHs for neural engineering remains a persistent challenge, demanding advancements in material innovation and hierarchical structural design.

2) *Multimodal hydrogel bioelectronics*: Neural recording and modulation technologies rely not only on electrical property but also on optical and chemical performances of hydrogel electronics. The integration of CHs with waveguide and/or drug-load design will be critical to develop multimodal neural interfacing based all-hydrogel bioelectronics. For instance, integrating controlled waveguide properties, such as transmittance and refractive index, with CHs enables closed-loop neural modulation. This synergy enables the hydrogel to record electrical signals and perform optogenetic stimulation, facilitating diagnosis and treatment through system-level all-hydrogel bioelectronics.[32b,134] Furthermore, CHs coupled with drug-controlled release system can achieve closed-loop neurotherapy. The neural signals recorded by CHs serve as feedback to initiate drug release in identified pathological conditions, with diseases predicted through real-time electrophysiological analysis.[135] Additionally, the complexity of the hydrogel electronics functionalities significantly increases the manufacturing difficulties. Multimodal hydrogel bioelectronics possessing diverse functionalities in a highly integrated manner will require further enhancement of current fabrication strategies.

3) *Wireless powered supply*: The power supply is a crucial component of neural biointerfacing technology. Current neural bioelectronics rely on external batteries or wired power sources, which are bulky and rigid, restricting their use in portable neural devices. Although soft and stretchable batteries have been developed, challenges with miniaturization and longevity continue to limit their application in implantable neural devices.[136] Recent advancements have demonstrated that wireless power supply systems offer an alternative solution for operating neural bioelectronics. These systems utilize technologies such as piezoelectricity,[137] radiofrequency,[111] and ultrasonic power transfer[138] to continuously deliver energy to implanted devices. CHs with integrated wireless power capabilities have been developed for this purpose. Examples include all-hydrogel batteries[139] and hydrogel nanogenerators,[140] which have been explored as power sources for implantable bioelectronics. However, ensuring the biosafety and biodegradability of these systems while integrating wireless power remains a critical challenge for current hydrogel bioelectronics. Therefore, innovation in biomaterials with wireless power designs has become a compelling area of research.

Conflict of Interest

The authors declare no conflict of interest.

Keywords

bioelectronics, biointerfacing, compliance, conducting hydrogels, neural engineering

[1] a) J. A. Frank, M.-J. Antonini, P. Anikeeva, *Nat. Biotechnol.* **2019**, *37*, 1013; b) Y. Park, T. S. Chung, G. Lee, J. A. Rogers, *Chem. Rev.* **2021**,

**ADVANCED
SCIENCE NEWS**

www.advancedsciencenews.com

**ADVANCED
FUNCTIONAL
MATERIALS**

www.afm-journal.de

122, 5277; c) H. Acarón Ledesma, X. Li, J. L. Carvalho-de-Souza, W. Wei, F. Bezanilla, B. Tian, *Nat. Nanotechnol.* **2019**, *14*, 645; d) B. Tian, C. M. Lieber, *Chem. Rev.* **2019**, *119*, 9136; e) R. Chen, A. Canales, P. Anikeeva, *Nat. Rev. Mater.* **2017**, *2*, 16093.

[2] a) U. Chaudhary, N. Birbaumer, A. Ramos-Murguialday, *Nat. Rev. Neurol.* **2016**, *12*, 513; b) M. S. Willsey, S. R. Nason-Tomaszewski, S. R. Ensel, H. Temmar, M. J. Mender, J. T. Costello, P. G. Patil, C. A. Chestek, *Nat. Commun.* **2022**, *13*, 6899.

[3] R. e. Gilron, S. Little, R. Perrone, R. Wilt, C. de Hemptinne, M. S. Yaroshinsky, C. A. Racine, S. S. Wang, J. L. Ostrem, P. S. Larson, D. D. Wang, N. B. Galifianakis, I. O. Bledsoe, M. San Luciano, H. E. Dawes, G. A. Worrell, V. Kremen, D. A. Borton, T. Denison, P. A. Starr, *Nat. Biotechnol.* **2021**, *39*, 1078.

[4] A. S. Ríos, S. Oxenford, C. Neudorfer, K. Butenko, N. Li, N. Rajamani, A. Boutet, G. J. B. Elias, J. Germann, A. Loh, W. Deeb, F. Wang, K. Setsompop, B. Salvato, L. B. d. Almeida, K. D. Foote, R. Amaral, P. B. Rosenberg, D. F. Tang-Wai, D. A. Wolk, A. D. Burke, S. Salloway, M. N. Sabbagh, M. M. Chakravarty, G. S. Smith, C. G. Lyketsos, M. S. Okun, W. S. Anderson, Z. Mari, F. A. Ponce, et al., *Nat. Commun.* **2022**, *13*, 7707.

[5] K. W. Scangos, A. N. Khambhati, P. M. Daly, G. S. Makhoul, L. P. Sugrue, H. Zamanian, T. X. Liu, V. R. Rao, K. K. Sellers, H. E. Dawes, P. A. Starr, A. D. Krystal, E. F. Chang, *Nat. Med.* **2021**, *27*, 1696.

[6] H. Shin, S. Jeong, J.-H. Lee, W. Sun, N. Choi, I.-J. Cho, *Nat. Commun.* **2021**, *12*, 492.

[7] T. Wang, M. Wang, J. Wang, L. Yang, X. Ren, G. Song, S. Chen, Y. Yuan, R. Liu, L. Pan, Z. Li, W. R. Leow, Y. Luo, S. Ji, Z. Cui, K. He, F. Zhang, F. Lv, Y. Tian, K. Cai, B. Yang, J. Niu, H. Zou, S. Liu, G. Xu, X. Fan, B. Hu, X. J. Loh, L. Wang, X. Chen, *Nat. Electron.* **2022**, *5*, 586.

[8] a) Y. H. Cho, Y. G. Park, S. Kim, J. U. Park, *Adv. Mater.* **2021**, *33*, 2005805; b) F. He, R. Lycke, M. Ganji, C. Xie, L. Luan, *iScience* **2020**, *23*, 8; c) J. Zhang, L. Wang, Y. Xue, I. M. Lei, X. Chen, P. Zhang, C. Cai, X. Liang, Y. Lu, J. Liu, *Adv. Mater.* **2022**, *35*, 2209324.

[9] a) J. Rivnay, L. Fenno, K. Deisseroth, G. Malliaras, *Sci. Adv.* **2017**, *3*, e1601649; b) G. Hong, C. M. Lieber, *Nat. Rev. Neurosci.* **2019**, *20*, 330.

[10] a) J. Luo, N. Xue, J. Chen, *Biosensors* **2022**, *12*, 1167; b) M. D. Serruya, J. P. Harris, D. O. Adewole, L. A. Struzyna, J. C. Burrell, A. Nemes, D. Petrov, R. H. Kraft, H. I. Chen, J. A. Wolf, D. K. Cullen, *Adv. Funct. Mater.* **2017**, *28*, 1701183.

[11] a) L. Luan, Z. Zhao, J. J. Siegel, O. Potnis, C. A. Tuppen, S. Lin, S. Kazmi, R. A. Fowler, S. Holloway, A. K. Dunn, R. A. Chitwood, C. Xie, *Sci. Adv.* **2017**, *3*, e1601966; b) J. J. Jun, N. A. Steinmetz, J. H. Siegle, D. J. Denman, M. Bauza, B. Barbarits, A. K. Lee, C. A. Anastassiou, A. Andrei, Ç. Aydın, M. Barbic, T. J. Blanche, V. Bonin, J. Couto, B. Dutta, S. L. Gratiy, D. A. Gutnisky, M. Häusser, B. Karsh, P. Ledochowitsch, C. M. Lopez, C. Mitelut, S. Musa, M. Okun, M. Pachitariu, J. Putzeys, P. D. Rich, C. Rossant, W.-l. Sun, K. Svoboda, et al., *Nature* **2017**, *551*, 232; c) J. W. Seo, K. Kim, K. W. Seo, M. K. Kim, S. Jeong, H. Kim, J. W. Ghim, J. H. Lee, N. Choi, J. Y. Lee, H. J. Lee, *Adv. Funct. Mater.* **2020**, *30*, 34.

[12] a) C. Sun, Z. Cheng, J. Abu-Halimah, B. Tian, *iScience* **2023**, *26*, 5; b) F. Vitale, D. G. Vercosa, A. V. Rodriguez, S. S. Pamulapati, F. Seibt, E. Lewis, J. S. Yan, K. Badhiwala, M. Adnan, G. Royer-Carfagni, M. Beierlein, C. Kemere, M. Pasquali, J. T. Robinson, *Nano Lett.* **2017**, *18*, 326.

[13] a) X. Dai, G. Hong, T. Gao, C. M. Lieber, *Acc. Chem. Res.* **2018**, *51*, 309; b) T. Zhou, G. Hong, T. M. Fu, X. Yang, T. G. Schuhmann, R. D. Viveros, C. M. Lieber, *Proc. Natl. Acad. Sci. U S A* **2017**, *114*, 5894; c) M. Kim, H. Lee, S. Nam, D.-H. Kim, G. D. Cha, *Acc. Chem. Res.* **2024**, *57*, 1633; d) G. Hong, X. Yang, T. Zhou, C. M. Lieber, *Curr. Opin. Neurobiol.* **2018**, *50*, 33.

[14] a) C. J. Bettinger, *Bioelectro. Med.* **2018**, *4*, 6. b) R. Jiao, R. Wang, Y. Wang, Y. K. Cheung, X. Chen, X. Wang, Y. Deng, H. Yu, *Microsyst. Nanoeng.* **2023**, *9*, 149; c) X. Tang, Y. He, J. Liu, *Biophys. Rev.* **2022**, *3*, 011301.

[15] a) J. I. Kim, D. H. Lee, B. Kim, Y.-K. Shin, S.-M. Kim, H. Lee, M.-H. Seo, J. Jeong, *ACS Appl. Electron. Mater.* **2023**, *5*, 2656; b) H. Park, S. Kim, J. Lee, K. Kim, H. Na, Y. Kim, D. Kim, D. Shin, B. Kim, K. Sim, *npj Flexible Electron.* **2024**, *8*, 63.

[16] J. Wu, J. Deng, G. Theocharidis, T. L. Sarrafian, L. G. Griffiths, R. T. Bronson, A. Veves, J. Chen, H. Yuk, X. Zhao, *Nature* **2024**, *630*, 360.

[17] a) H. Tang, Y. Li, S. Liao, H. Liu, Y. Qiao, J. Zhou, *Adv. Healthcare Mater.* **2024**, *13*, 2313953; b) Y. Hui, Y. Yao, Q. Qian, J. Luo, H. Chen, Z. Qiao, Y. Yu, L. Tao, N. Zhou, *Nat. Electron.* **2022**, *5*, 893; c) H. Yuk, B. Lu, S. Lin, K. Qu, J. Xu, J. Luo, X. Zhao, *Nat. Commun.* **2020**, *11*, 1604; d) H. Yuk, J. Wu, X. Zhao, *Nat. Rev. Mater.* **2022**, *7*, 935; e) Q. Yang, Z. Hu, J. A. Rogers, *Acc. Mater. Res.* **2021**, *2*, 1010. f) X. Liu, J. Liu, S. Lin, X. Zhao, *Mater. Today* **2020**, *36*, 102.

[18] a) X. He, D. Liu, B. Cui, H. Huang, S. Dai, I. Pang, Y. Qiao, T. Xu, S. Zhang, *Adv. Funct. Mater.* **2024**, *34*, 2405896; b) Z. Li, J. Lu, T. Ji, Y. Xue, L. Zhao, K. Zhao, B. Jia, B. Wang, J. Wang, S. Zhang, Z. Jiang, *Adv. Mater.* **2024**, *36*, 2306350; c) C. Xie, X. Wang, H. He, Y. Ding, X. Lu, *Adv. Funct. Mater.* **2020**, *30*, 1909954; d) G. Li, K. Huang, J. Deng, M. Guo, M. Cai, Y. Zhang, C. F. Guo, *Adv. Mater.* **2022**, *34*, 2200261.

[19] a) A. Motealleh, N. S. Kehr, *Adv. Healthcare Mater.* **2017**, *6*, 1600938; b) X. Xue, X. Hu, Y. Deng, J. Su, *Adv. Funct. Mater.* **2021**, *31*, 2009432.

[20] a) T.-C. Ho, C.-C. Chang, H.-P. Chan, T.-W. Chung, C.-W. Shu, K.-P. Chuang, T.-H. Duh, M.-H. Yang, Y.-C. Tyan, *Molecules* **2022**, *27*, 2902; b) M. Yang, L. Wang, W. Liu, W. Li, Y. Huang, Q. Jin, L. Zhang, Y. Jiang, Z. Luo, *Nat. Commun.* **2024**, *15*, 7993.

[21] C. W. Zhang, C. Chen, S. Duan, Y. Yan, P. He, X. He, *Med-X* **2024**, *2*, 20.

[22] Q. Liang, X. Xia, X. Sun, D. Yu, X. Huang, G. Han, S. M. Mugo, W. Chen, Q. Zhang, *Adv. Sci.* **2022**, *9*, 2201059.

[23] a) C. Xu, Y. Chang, P. Wu, K. Liu, X. Dong, A. Nie, C. Mu, Z. Liu, H. Dai, Z. Luo, *Adv. Funct. Mater.* **2021**, *31*, 2104440; b) C. Xu, Y. Xu, M. Yang, Y. Chang, A. Nie, Z. Liu, J. Wang, Z. Luo, *Adv. Funct. Mater.* **2020**, *30*, 2000177.

[24] a) X. Tang, H. Shen, S. Zhao, N. Li, J. Liu, *Nat. Electron.* **2023**, *6*, 109; b) J. Wang, T. Wang, H. Liu, K. Wang, K. Moses, Z. Feng, P. Li, W. Huang, *Adv. Mater.* **2023**, *35*, 2211012.

[25] S. M. Won, E. Song, J. Zhao, J. Li, J. Rivnay, J. A. Rogers, *Adv. Mater.* **2018**, *30*, 1800534.

[26] a) W. Duan, U. A. Robles, L. Poole-Warren, D. Esrafilzadeh, *Adv. Sci.* **2023**, *11*, 2306275; b) G. T. Go, Y. Lee, D. G. Seo, T. W. Lee, *Adv. Mater.* **2022**, *34*, 2270311.

[27] a) H. Yuk, B. Lu, X. Zhao, *Chem. Soc. Rev.* **2019**, *48*, 1642; b) C. Yang, Z. Suo, *Nat. Rev. Mater.* **2018**, *3*, 125; c) L. Hu, P. L. Chee, S. Sugiarto, Y. Yu, C. Shi, R. Yan, Z. Yao, X. Shi, J. Zhi, D. Kai, H. D. Yu, W. Huang, *Adv. Mater.* **2023**, *35*, 2205326.

[28] Y. Xue, X. Chen, F. Wang, J. Lin, J. Liu, *Adv. Mater.* **2023**, *35*, 2304095.

[29] M. Lee, Y. Lee, J. H. Choi, H. Kim, D. Jeong, K. Park, J. Kim, J. Park, W. Y. Jang, J. Seo, J. Lee, *ACS Nano* **2024**, *18*, 12210.

[30] M. Jia, M. Rolandi, *Adv. Healthcare Mater.* **2020**, *9*, 1901372.

[31] R. Ji, S. Yan, S. Zhu, Y. Wang, D. He, K. Wang, D. Zhou, Q. Jia, X. Wang, B. Zhang, C. Shi, T. Xu, R. Wang, R. Wang, Y. Zhou, *Adv. Sci.* **2024**, *11*, e2401869.

[32] a) S. Chen, J. Duan, M. Jaroniec, S. Z. Qiao, *Adv. Mater.* **2014**, *26*, 2925; b) S. Huang, X. Liu, S. Lin, C. Glynn, K. Felix, A. Sahasrabudhe, C. Maley, J. Xu, W. Chen, E. Hong, A. J. Crosby, Q. Wang, S. Rao, *Nat. Commun.* **2024**, *15*, 3525.

[33] J. Park, J. Jeon, B. Kim, M. S. Lee, S. Park, J. Lim, J. Yi, H. Lee, H. S. Yang, J. Y. Lee, *Adv. Funct. Mater.* **2020**, *30*, 2003759.

[34] P. GhavamiNejad, A. GhavamiNejad, H. Zheng, K. Dhingra, M. Samarikhalaj, M. Poudineh, *Adv. Healthcare Mater.* **2022**, *12*, 2202362.

**ADVANCED
SCIENCE NEWS**

www.advancedsciencenews.com

**ADVANCED
FUNCTIONAL
MATERIALS**

www.afm-journal.de

[35] S. Gong, X. Zhang, X. A. Nguyen, Q. Shi, F. Lin, S. Chauhan, Z. Ge, W. Cheng, *Nat. Nanotechnol.* **2023**, *18*, 889.

[36] Y. Zhao, K. Zhao, R. Qian, Z. Yu, C. Ye, *Chem. Eng. J.* **2024**, *486*, 150197.

[37] D. Song, X. Li, M. Jang, Y. Lee, Y. Zhai, W. Hu, H. Yan, S. Zhang, L. Chen, C. Lu, K. Kim, N. Liu, *Adv. Mater.* **2023**, *35*, 2304956.

[38] M. T. Rahman, M. S. Rahman, H. Kumar, K. Kim, S. Kim, *Adv. Funct. Mater.* **2023**, *33*, 2303471.

[39] Z. Wei, J. H. Yang, J. Zhou, F. Xu, M. Zrinyi, P. H. Dussault, Y. Osada, Y. M. Chen, *Chem. Soc. Rev.* **2014**, *43*, 8114.

[40] a) B. Lu, H. Yuk, S. Lin, N. Jian, K. Qu, J. Xu, X. Zhao, *Nat. Commun.* **2019**, *10*, 1043; b) G. Li, *Soft Science* **2022**, *2*; c) J. Lin, X. Chen, P. Zhang, Y. Xue, Y. Feng, Z. Ni, Y. Tao, Y. Wang, J. Liu, *Adv. Mater.* **2024**, *36*, 2400181; d) Y. Xue, J. Zhang, X. Chen, J. Zhang, G. Chen, K. Zhang, J. Lin, C. Guo, J. Liu, *Adv. Funct. Mater.* **2021**, *31*, 2106446.

[41] Y. Zhou, C. Wan, Y. Yang, H. Yang, S. Wang, Z. Dai, K. Ji, H. Jiang, X. Chen, Y. Long, *Adv. Funct. Mater.* **2018**, *29*, 1806220.

[42] a) Y. Liu, C. Wang, J. Xue, G. Huang, S. Zheng, K. Zhao, J. Huang, Y. Wang, Y. Zhang, T. Yin, Z. Li, *Adv. Healthcare Mater.* **2022**, *11*, e2200653; b) C. Wang, Y. Liu, X. Qu, B. Shi, Q. Zheng, X. Lin, S. Chao, C. Wang, J. Zhou, Y. Sun, G. Mao, Z. Li, *Adv. Mater.* **2022**, *34*, 2270122.

[43] a) Y. Ohm, C. Pan, M. J. Ford, X. Huang, J. Liao, C. Majidi, *Nat. Electron.* **2021**, *4*, 185; b) H. Wang, T. Zhuang, J. Wang, X. Sun, Y. Wang, K. Li, X. Dai, Q. Guo, X. Li, D. Chong, B. Chen, J. Yan, *Adv. Mater.* **2023**, *35*, 2302919.

[44] M. Hu, J. Ren, Y. Pan, L. Cheng, X. Xu, C. L. Tan, H. Sun, Y. Shi, S. Yan, *Adv. Funct. Mater.* **2024**, *34*, 2407926.

[45] M. Liu, W. Zhang, S. Han, D. Zhang, X. Zhou, X. Guo, H. Chen, H. Wang, L. Jin, S. Feng, Z. Wei, *Adv. Mater.* **2024**, *36*, 2313672.

[46] L. Han, X. Lu, M. Wang, D. Gan, W. Deng, K. Wang, L. Fang, K. Liu, C. W. Chan, Y. Tang, L. T. Weng, H. Yuan, *Small* **2017**, *13*, 1601916.

[47] M. Yang, P. Chen, X. Qu, F. Zhang, S. Ning, L. Ma, K. Yang, Y. Su, J. Zang, W. Jiang, T. Yu, X. Dong, Z. Luo, *ACS Nano* **2023**, *17*, 885.

[48] B. Worfolk, S. Andrews, S. Park, J. Reinspach, N. Liu, M. Toney, S. B. Mannsfeld, Z. Bao, *Proc. Natl. Acad. Sci. USA* **2015**, *112*, 14138.

[49] Y. Liu, J. Liu, S. Chen, T. Lei, Y. Kim, S. Niu, H. Wang, X. Wang, A. M. Foudeh, J. B. H. Tok, Z. Bao, *Nat. Biomed. Eng.* **2019**, *3*, 58.

[50] Y. Guo, P.-C. Shen, C. Su, A.-Y. Lu, M. Hempel, Y. Han, Q. Ji, Y. Lin, E. Shi, E. McVay, L. Dou, D. A. Muller, T. Palacios, J. Li, X. Ling, J. Kong, *Proc. Natl. Acad. Sci. USA* **2019**, *116*, 3437.

[51] W. Mei, Z. Zhang, A. Zhang, D. Li, X. Zhang, H. Wang, Z. Chen, Y. Li, X. Li, X. Xu, *Nano Res.* **2020**, *13*, 2485.

[52] A. Mironov, J. Kim, Y. Huang, A. Steinforth, D. Sievers, J. Eden, *Nanoscale* **2020**, *12*, 16796.

[53] Y. Jiang, Z. Zhang, Y. Wang, D. Li, C. Coen, E. Hwaun, G. Chen, H. Wu, D. Zhong, S. Niu, W. Wang, A. Saberi, J. Lai, Y. Wu, Y. Wang, A. A. Trotsyuk, K. Y. Loh, C. Shih, W. Xu, K. Liang, K. Zhang, Y. Bai, G. Gurusankar, W. Hu, W. Jia, Z. Cheng, R. H. Dauskardt, G. C. Gurtner, J. B. Tok, K. Deisseroth, et al., *Science* **2022**, *375*, 1411.

[54] P. Zhu, Q. Song, S. Bhagwat, F. Mayoussi, A. Goralczyk, N. Nekoonam, M. Sanjaya, P. Hou, S. Tisato, F. Kotz-Helmer, D. Helmer, B. E. Rapp, *Nat. Commun.* **2024**, *15*, 5673.

[55] a) J. Hsieh, W. He, D. Venkatraghavan, V. B. Koptelova, Z. J. Ahmad, I. Pyatnitskiy, W. Wang, J. Jeong, K. K. W. Tang, C. Harmeier, C. Li, M. Rana, S. Iyer, E. Nayak, H. Ding, P. Modur, V. Mysliwiec, D. M. Schnyer, B. Baird, H. Wang, *Device* **2024**, *2*, 100182; b) Q. Han, C. Zhang, T. Guo, Y. Tian, W. Song, J. Lei, Q. Li, A. Wang, M. Zhang, S. Bai, X. Yan, *Adv. Mater.* **2023**, *35*, 2209606.

[56] Y. Liu, H. Zhou, W. Zhou, S. Meng, C. Qi, Z. Liu, T. Kong, *Adv. Energy Mater.* **2021**, *11*, 2101329.

[57] H. He, H. Li, A. Pu, W. Li, K. Ban, L. Xu, *Nat. Commun.* **2023**, *14*, 759.

[58] J. E. Park, H. S. Kang, M. Koo, C. Park, *Adv. Mater.* **2020**, *32*, 2002178.

[59] a) H. Qin, Y. Yan, Q. Feng, H. Liu, H. Cong, S. Yu, *Nano Lett.* **2022**, *22*, 8101; b) K. Tao, Z. Chen, J. Yu, H. Zeng, J. Wu, Z. Wu, Q. Jia, P. Li, Y. Fu, H. Chang, W. Yuan, *Adv. Sci.* **2022**, *9*, 2104168.

[60] a) Y. Lu, G. Yang, S. Wang, Y. Zhang, Y. Jian, L. He, T. Yu, H. Luo, D. Kong, Y. Xianyu, B. Liang, T. Liu, X. Ouyang, J. Yu, X. Hu, H. Yang, Z. Gu, W. Huang, K. Xu, *Nat. Electron.* **2023**, *7*, 51; b) K. Unger, F. Greco, A. M. Coclite, *Adv. Mater. Technol.* **2021**, *7*, 2100717.

[61] M. Shur, F. Fallegger, E. Pirondini, A. Roux, A. Bichat, Q. Barraud, G. Courtine, S. P. Lacour, *ACS Appl. Bio Mater.* **2020**, *3*, 4388.

[62] S. Zheng, H. Wang, P. Das, Y. Zhang, Y. Cao, J. Ma, S. Liu, Z. S. Wu, *Adv. Mater.* **2021**, *33*, 2005449.

[63] M. Zhang, Y. Lee, Z. Zheng, M. T. A. Khan, X. Lyu, J. Byun, H. Giessen, M. Sitti, *Nat. Commun.* **2023**, *14*, 8208.

[64] D. Won, J. Kim, J. Choi, H. Kim, S. Han, I. Ha, J. Bang, K. K. Kim, Y. Lee, T. Kim, J. Park, C. Kim, S. H. Ko, *Sci. Adv.* **2022**, *8*, eabo3209.

[65] R. Miyakoshi, S. Hayashi, M. Terakawa, *Adv. Electron. Mater.* **2023**, *9*, 2201277.

[66] a) Y. Li, H. Zhou, H. Yang, K. Xu, *Nano-Micro Lett.* **2024**, *17*, 57; b) D. Won, H. Kim, J. Kim, H. Kim, M. W. Kim, J. Ahn, K. Min, Y. Lee, S. Hong, J. Choi, C. Y. Kim, T. Kim, S. H. Ko, *Nat. Electron.* **2024**, *7*, 475.

[67] X. Xie, Z. Xu, X. Yu, H. Jiang, H. Li, W. Feng, *Nat. Commun.* **2023**, *14*, 4289.

[68] F. Wang, Y. Xue, X. Chen, P. Zhang, L. Shan, Q. Duan, J. Xing, Y. Lan, B. Lu, J. Liu, *Adv. Funct. Mater.* **2023**, *34*, 2314471.

[69] T. Zhou, H. Yuk, F. Hu, J. Wu, F. Tian, H. Roh, Z. Shen, G. Gu, J. Xu, B. Lu, X. Zhao, *Nat. Mater.* **2023**, *22*, 895.

[70] a) S. Liu, Y. Rao, H. Jang, P. Tan, N. Lu, *Matter* **2022**, *5*, 1104; b) I. Dimov, M. Moser, G. Malliaras, I. McCulloch, *Chem. Rev.* **2022**, *122*, 4356.

[71] a) M. Yan, L. Wang, Y. Wu, X. Liao, C. Zhong, L. Wang, Y. Lu, *ACS Appl. Mater. Interfaces* **2023**, *15*, 41310; b) M. Han, E. Yildiz, H. Kaleli, S. Karaz, G. Eren, I. Dogru-Yuksel, E. Senses, A. Sahin, S. Nizamoglu, *Adv. Health. Mater.* **2022**, *11*, 2102160; c) X. Ren, W. Bai, S. Chen, Y. Yuan, X. Shao, X. Zhu, L. Wang, Q. Jiang, B. Hu, *npj Flex. Electron.* **2024**, *8*, 36; d) Y. Fang, X. Yang, Y. Lin, J. Shi, A. Prominski, C. Clayton, E. Ostroff, B. Tian, *Chem. Rev.* **2021**, *122*, 5233; e) J. Yi, G. Zou, J. Huang, X. Ren, Q. Tian, Q. Yu, P. Wang, Y. Yuan, W. Tang, C. Wang, *Nature* **2023**, *624*, 295; f) H. Li, H. Liu, M. Sun, Y. Huang, L. Xu, *Adv. Mater.* **2021**, *33*, 2004425; g) W. Tang, Y. Zhou, S. Chen, S. Yu, Y. Yang, J. Lin, S. Yin, Y. Ma, B. Hu, *ACS Mater. Lett.* **2021**, *3*, 1385.

[72] a) C. Wang, X. Chen, L. Wang, M. Makihata, H. Liu, T. Zhou, X. Zhao, *Science* **2022**, *366*, 517; b) J. Deng, H. Yuk, J. Wu, C. Varela, X. Chen, E. Roche, C. Guo, X. Zhao, *Nat. Mater.* **2020**, *20*, 229.

[73] J. Chong, C. Sung, K. S. Nam, T. Kang, H. Kim, H. Lee, H. Park, S. Park, J. Kang, *Nat. Commun.* **2023**, *14*, 2206.

[74] H. Yuk, C. Varela, C. Nabzdyk, X. Mao, R. Padera, E. Roche, X. Zhao, *Nature* **2019**, *575*, 169.

[75] K. Zhang, X. Chen, Y. Xue, J. Lin, X. Liang, J. Zhang, J. Zhang, G. Chen, C. Cai, J. Liu, *Adv. Funct. Mater.* **2021**, *32*, 2111465.

[76] H. Yuk, T. Zhang, S. Lin, G. A. Parada, X. Zhao, *Nat. Mater.* **2015**, *15*, 190.

[77] a) Z. Liu, F. Yan, *Adv. Sci.* **2022**, *9*, 2200264.; b) X. Chen, H. Yuk, J. Wu, C. Nabzdyk, X. Zhao, *Proc. Natl. Acad. Sci. USA* **2020**, *117*, 15497.

[78] a) Y. Zhang, G. Lee, S. Li, Z. Hu, K. Zhao, J. A. Rogers, *Chem. Rev.* **2023**, *123*, 11722; b) K. Yu, D. Kuzum, S.-W. Hwang, B. Kim, H. Juul, N. Kim, S. Won, K. Chiang, M. Trumpis, A. Richardson, H. Cheng, H. Fang, M. Thompson, H. Bink, D. Talos, K. Seo, H. Lee, S.-K. Kang, J.-H. Kim, J. Lee, Y. Huang, F. Jensen, M. Dichter, T. Lucas, J. Viventi, B. Litt, J. A. Rogers, *Nat. Mater.* **2016**, *15*, 782; c) Y. Huang, K. Yao, Q. Zhang, X. Huang, Z. Chen, Y. Zhou, X. Yu, *Chem. Soc. Rev.* **2024**, *53*, 8632.

[79] a) C. Li, C. Guo, V. Fitzpatrick, A. Ibrahim, M. Zwierstra, P. Hanna, A. Lechtig, A. Nazarian, S. Lin, D. Kaplan, *Nat. Rev. Mater.* **2019**, *5*, 61; b) P. Kharkar, K. Kiick, A. Kloxin, *Chem. Soc. Rev.* **2013**, *42*, 7335.

[80] a) X. Lin, C. Tsao, M. Kyomoto, M. Zhang, *Adv. Healthcare Mater.* **2021**, *11*, 2101479.; b) K. Zhang, Q. Feng, Z. Fang, L. Gu, L. Bian, *Chem. Rev.* **2021**, *121*, 11149.

[81] a) D. Zauchner, M. Müller, M. Horrer, L. Bissig, F. Zhao, P. Fisch, S. Lee, M. Zenobi-Wong, R. Müller, X.-H. Qin, *Nat. Commun.* **2024**, *15*, 5027.; b) E. Zant, D. Grijpma, *Biomacromolecules* **2016**, *17*, 1582.

[82] X. Li, L. He, Y. Li, M. Chao, M. Li, P. Wan, L. Zhang, *ACS Nano* **2021**, *15*, 7765.

[83] a) Y. Wang, H. Haick, S. Guo, C. Wang, S. Lee, T. Yokota, T. Someya, *Chem. Soc. Rev.* **2022**, *51*, 3759; b) Y. Li, N. Li, N. De Oliveira, S. Wang, *Matter* **2021**, *4*, 1125; c) J. Goding, A. Gilmour, U. Aregueta-Robles, E. Hasan, R. Green, *Adv. Funct. Mater.* **2017**, *28*, 1702969; d) A. Bos, A. Carnicer-Lombarte, A. Güemes-Gonzalez, D. van Niekerk, S. Hilton, D. Barone, C. Proctor, R. Owens, G. Malliaras, *Adv. Mater.* **2022**, *35*, 2207847.

[84] J. Park, Y. Lee, T. Kim, S. Hwang, J. Seo, *ACS Appl. Electron. Mater.* **2022**, *4*, 1449.

[85] a) L. Li, M. Yue, Q. Peng, X. Pu, Z. Li, *Adv. Funct. Mater.* **2023**, *34*, 2309594; b) Y. Zhao, N. Yang, X. Chu, F. Sun, M. Ali, Y. Zhang, B. Yang, Y. Cai, M. Liu, N. Gasparini, J. Zheng, C. Zhang, C. Guo, H. Meng, *Adv. Mater.* **2023**, *35*, 2211617; c) Z. Pan, J. Dorogin, A. Lofts, G. Randhawa, F. Xu, R. Slick, M. Abraha, C. Tran, M. Lawlor, T. Hoare, *Adv. Healthcare Mater.* **2024**, *13*, 2304397; d) P. Zhang, I. Lei, G. Chen, J. Lin, X. Chen, J. Zhang, C. Cai, X. Liang, J. Liu, *Nat. Commun.* **2022**, *13*, 4775.

[86] a) I. Han, K. Song, S. Jung, Y. Jo, J. Kwon, T. Chung, S. Yoo, J. Jang, Y. Kim, D. Hwang, Y. Kim, *Adv. Mater.* **2022**, *35*, 2203431; b) X. Xia, Q. Liang, X. Sun, D. Yu, X. Huang, S. M. Mugo, W. Chen, D. Wang, Q. Zhang, *Adv. Funct. Mater.* **2022**, *32*, 2208024; c) G. Tian, D. Yang, C. Liang, Y. Liu, J. Chen, Q. Zhao, S. Tang, J. Huang, P. Xu, Z. Liu, D. Qi, *Adv. Mater.* **2023**, *35*, 2212302.

[87] X. Li, K. Cui, T. L. Sun, L. Meng, C. Yu, L. Li, C. Creton, T. Kurokawa, J. Gong, *Proc. Natl. Acad. Sci. USA* **2020**, *117*, 7606.

[88] M. Li, H. Lu, M. Pi, H. Zhou, Y. Wang, B. Yan, W. Cui, R. Ran, *Adv. Sci.* **2023**, *10*, 2304780.

[89] a) S. Lin, H. Yuk, T. Zhang, G. A. Parada, H. Koo, C. Yu, X. Zhao, *Adv. Mater.* **2015**, *28*, 4497; b) H. Yuk, T. Zhang, G. A. Parada, X. Liu, X. Zhao, *Nat. Commun.* **2016**, *7*, 12028.

[90] J. H. Weerd, V. M. Christoffels, *Development* **2016**, *143*, 197.

[91] a) F. W. Prinzen, A. Auricchio, W. Mullens, C. Linde, J. F. Huizar, *Eur. Heart J.* **2022**, *43*, 1917; b) M. K. Lahiri, P. J. Kannankeril, J. J. Goldberger, *J. Am. Coll. Cardiol.* **2008**, *51*, 1725.

[92] S. I. Han, S. Sunwoo, C. S. Park, S. Lee, T. Hyeon, D. Kim, *ACS Nano* **2024**, *18*, 12025.

[93] a) J. Keiler, M. Schulze, M. Sombetzki, T. Heller, T. Tischer, N. Grabow, A. Wree, D. Bänsch, *J. Cardiol.* **2017**, *70*, 7; b) A. S. Varshney, E. M. DeFilippis, J. A. Cowger, I. Netuka, S. P. Pinney, M. M. Givertz, *J. Am. Coll. Cardiol.* **2022**, *79*, 1092.

[94] S. Sunwoo, S. Han, C. Park, J. Kim, J. Georgiou, S. Lee, D. Kim, T. Hyeon, *Nat. Rev. Bioeng.* **2023**, *2*, 8.

[95] J. Zhang, S. Shen, R. Lin, J. Huang, C. Pu, P. Chen, Q. Duan, X. You, C. Xu, B. Yan, X. Gao, Z. Shen, L. Cai, X. Qiu, H. Hou, *Adv. Mater.* **2023**, *35*, 2209497.

[96] C. Yu, M. Shi, S. He, M. Yao, H. Sun, Z. Yue, Y. Qiu, B. Liu, L. Liang, Z. Zhao, F. Yao, H. Zhang, J. Li, *Nat. Commun.* **2023**, *14*, 6226.

[97] H. Choi, Y. Kim, S. Kim, H. Jung, S. Lee, K. Kim, H. Han, J. Y. Kim, M. Shin, D. Son, *Nat. Electron.* **2023**, *6*, 779.

[98] E. T. Roche, M. A. Horvath, I. Wamala, A. Alazmani, S. Song, W. Whyte, Z. Machaidze, C. J. Payne, J. C. Weaver, G. Fishbein, J. Kuebler, N. V. Vasilyev, D. J. Mooney, F. A. Pigula, C. J. Walsh, *Sci. Transl. Med.* **2017**, *9*, eaaf3925.

[99] J. Liu, X. Zhang, Y. Liu, M. Rodrigo, P. D. Loftus, J. Aparicio-Valenzuela, J. Zheng, T. Pong, K. J. Cyr, M. Babakhanian, J. Hasi, J. Li, Y. Jiang, C. J. Kenney, P. J. Wang, A. M. Lee, Z. Bao, *Proc. Natl. Acad. Sci. USA* **2020**, *117*, 14769.

[100] S. Jin, H. Choi, D. Seong, C. L. You, J. S. Kang, S. Rho, W. B. Lee, D. Son, M. Shin, *Nature* **2023**, *623*, 58.

[101] W. Lei, C. Peng, S. Chiu, H. Lu, C. Wu, T. Cheng, W. Huang, *Adv. Funct. Mater.* **2023**, *34*, 2307365.

[102] M. Fakhoury, *Rev. Neurosci.* **2015**, *26*, 397.

[103] M. T. Filbin, *Nat. Rev. Neurosci.* **2003**, *4*, 703.

[104] S. A. Busch, J. Silver, *Curr. Opin. Neurobiol.* **2007**, *17*, 120.

[105] a) H. Durgam, S. Sapp, C. Deister, Z. Khaing, E. Chang, S. Luebben, C. E. Schmidt, *J. Biomater. Sci.* **2012**, *21*, 1265; b) P. M. George, A. W. Lyckman, D. A. LaVan, A. Hegde, Y. Leung, R. Avasare, C. Testa, P. M. Alexander, R. Langer, M. Sur, *Biomaterials* **2005**, *26*, 3511.

[106] M. Zeng, J. Ding, Y. Tian, Y. Zhang, X. Liu, Z. Chen, J. Sun, C. Wu, H. Yin, D. Wei, H. Fan, *Mater. Horiz.* **2024**, *11*, 6423.

[107] Z. Shen, Q. Liang, Q. Chang, Y. Liu, Q. Zhang, *Adv. Mater.* **2024**, *36*, 2310365.

[108] I. R. Minev, P. Musienko, A. Hirsch, Q. Barraud, N. Wenger, E. M. Moraud, J. Gandar, M. Capogrosso, T. Milekovic, L. Asboth, R. F. Torres, N. Vachicouras, Q. Liu, N. Pavlova, S. Duis, A. Larmagnac, J. Vörös, S. Micera, Z. Suo, G. Courtine, S. P. Lacour, *Science* **2015**, *347*, 159.

[109] S. Park, H. Yuk, R. Zhao, Y. S. Yim, E. W. Woldeghebriel, J. Kang, A. Canales, Y. Fink, G. B. Choi, X. Zhao, P. Anikeeva, *Nat. Commun.* **2021**, *12*, 3435.

[110] J. Shin, Y. Yan, W. Bai, Y. Xue, P. Gamble, L. Tian, I. Kandela, C. R. Haney, W. Spees, Y. Lee, M. Choi, J. Ko, H. Ryu, J. Chang, M. Pezhouh, S. Kang, S. M. Won, K. J. Yu, J. Zhao, Y. K. Lee, M. R. MacEwan, S. Song, Y. Huang, W. Z. Ray, J. A. Rogers, *Nat. Biomed. Eng.* **2018**, *3*, 37.

[111] J. Koo, M. R. MacEwan, S. Kang, S. M. Won, M. Stephen, P. Gamble, Z. Xie, Y. Yan, Y. Chen, J. Shin, N. Birenbaum, S. Chung, S. B. Kim, J. Khalifeh, D. V. Harburg, K. Bean, M. Paskett, J. Kim, Z. S. Zohny, S. M. Lee, R. Zhang, K. Luo, B. Ji, A. Banks, H. M. Lee, Y. Huang, W. Z. Ray, J. A. Rogers, *Nat. Med.* **2018**, *24*, 1830.

[112] Y. Dai, M. Du, L. Huang, J. Zheng, L. Wei, J. Qiu, C. Ren, S. Zhou, *Adv. Opt. Mater.* **2022**, *11*, 2202184.

[113] G. D. Spyropoulos, J. Savarin, E. F. Gomez, D. T. Simon, M. Berggren, J. N. Gelinas, E. Stavrinidou, D. Khodagholy, *Adv. Mater. Technol.* **2019**, *5*, 1900652.

[114] Z. Zhang, B. Sabbagh, Y. Chen, G. Yossifon, *ACS Nano* **2024**, *18*, 15025.

[115] L. Wang, S. Wang, G. Xu, Y. Qu, H. Zhang, W. Liu, J. Dai, T. Wang, Z. Liu, Q. Liu, K. Xiao, *ACS Nano* **2024**, *18*, 29704.

[116] J. Yang, R. Wang, Y. Ren, J. Mao, Z. Wang, Y. Zhou, S. Han, *Adv. Mater.* **2020**, *32*, 2003610.

[117] J. M. Sabandal, J. A. Berry, R. L. Davis, *Nature* **2021**, *591*, 426.

[118] V. K. Sangwan, M. C. Hersam, *Nat. Nanotechnol.* **2020**, *15*, 517.

[119] J. Yan, J. P. Armstrong, F. Scarpa, A. W. Perriman, *Adv. Mater.* **2024**, *36*, 2403937.

[120] W. Liu, T. Mei, Z. Cao, C. Li, Y. Wu, L. Wang, G. Xu, Y. Chen, Y. Zhou, S. Wang, Y. Xue, Y. Yu, X. Kong, R. Chen, B. Tu, K. Xiao, *Sci. Adv.* **2024**, *10*, eadj7867.

[121] a) S. Dai, Y. Dai, Z. Zhao, F. Xia, Y. Li, Y. Liu, P. Cheng, J. Strzalka, S. Li, N. Li, Q. Su, S. Wai, W. Liu, C. Zhang, R. Zhao, J. Yang, R. Stevens, J. Xu, J. Huang, S. Wang, *Matter* **2022**, *5*, 3375; b) J. Hu, M. Jing, Y. Huang, B. Kou, Z. Li, Y. Xu, S. Yu, X. Zeng, J. Jiang, P. Lin, W. Zhao, *Adv. Mater.* **2024**, *36*, 2405887.

[122] H. Tang, Y. Li, B. Chen, X. Chen, Y. Han, M. Guo, H. Q. Xia, R. Song, X. Zhang, J. Zhou, *ACS Nano* **2022**, *16*, 17931.

[123] J. Wu, J. Xian, C. He, H. Lin, J. Li, F. Li, *Adv. Mater.* **2024**, *36*, 2405372.

**ADVANCED
SCIENCE NEWS**

www.advancedsciencenews.com

**ADVANCED
FUNCTIONAL
MATERIALS**

www.afm-journal.de

[124] Z. Leng, P. Zhu, X. Wang, Y. Wang, P. Li, W. Huang, B. Li, R. Jin, N. Han, J. Wu, Y. Mao, *Adv. Funct. Mater* **2023**, *33*, 2211056.

[125] L. Chen, Z. Wang, Z. Zhan, M. Xie, G. Duan, P. Cheng, Y. Chen, H. Duan, *Mater. Today Phys.* **2021**, *19*, 100404.

[126] A. Chortos, J. Liu, Z. Bao, *Nat. Mater.* **2016**, *15*, 937.

[127] Y. Shin, H. S. Lee, Y. J. Hong, S. H. Sunwoo, O. K. Park, S. H. Choi, D. H. Kim, S. Lee, *Sci. Adv.* **2024**, *10*, eadi7724.

[128] a) W. Guo, M. Ma, *J. Mater. Chem. A* **2024**, *12*, 9371; b) D. Boateng, X. Li, Y. Zhu, H. Zhang, M. Wu, J. Liu, Y. Kang, H. Zeng, L. Han, *Biosens. Bioelectron.* **2024**, *261*, 116499.

[129] a) Y. Feng, Y. Wang, C. Chen, Z. Wang, J. Liu, *Innov. Mater.* **2024**, *2*, 100105; b) H. Yang, M. Ji, M. Yang, M. Shi, Y. Pan, Y. Zhou, H. J. Qi, Z. Suo, J. Tang, *Matter* **2021**, *4*, 1935.

[130] J. Steck, J. Kim, Y. Kutsovsky, Z. Suo, *Nature* **2023**, *624*, 303.

[131] X. Liang, G. Chen, S. Lin, J. Zhang, L. Wang, P. Zhang, Z. Wang, Z. Wang, Y. Lan, Q. Ge, J. Liu, *Adv. Mater.* **2021**, *33*, 2102011.

[132] S. Lin, J. Liu, X. Liu, X. Zhao, *Proc. Natl. Acad. Sci. USA* **2019**, *116*, 10244.

[133] Z. Zhang, G. Chen, Y. Xue, Q. Duan, X. Liang, T. Lin, Z. Wu, Y. Tan, Q. Zhao, W. Zheng, L. Wang, F. Wang, X. Luo, J. Xu, J. Liu, B. Lu, *Adv. Funct. Mater.* **2023**, *33*, 2305705.

[134] X. Chen, Y. Feng, P. Zhang, Z. Ni, Y. Xue, J. Liu, *Adv. Mater.* **2024**, 2413476.

[135] J. Qu, K. Xie, S. Chen, X. He, Y. Wang, M. Chamberlin, X. Zhao, G. Zhu, C. Xu, P. Shi, *Sci. Adv.* **2024**, *10*, eadq9207.

[136] L. Dong, L. Shan, Y. Wang, J. Liu, *Supramol. Mater.* **2025**, *4*, 100082.

[137] E. J. Curry, T. T. Le, R. Das, K. Ke, E. M. Santorella, D. Paul, M. T. Chorsi, K. T. M. Tran, J. Baroody, E. R. Borges, B. Ko, A. Golabchi, X. Xin, D. Rowe, L. Yue, J. Feng, M. D. Morales-Acosta, Q. Wu, I. P. Chen, X. T. Cui, J. Pachter, T. D. Nguyen, *Proc. Natl. Acad. Sci. USA* **2020**, *117*, 214.

[138] D. M. Lee, M. Kang, I. Hyun, B. J. Park, H. J. Kim, S. H. Nam, H. J. Yoon, H. Ryu, H. M. Park, B. O. Choi, S. W. Kim, *Nat. Commun.* **2023**, *14*, 7315.

[139] T. Ye, J. Wang, Y. Jiao, L. Li, E. He, L. Wang, Y. Li, Y. Yun, D. Li, J. Lu, H. Chen, Q. Li, F. Li, R. Gao, H. Peng, Y. Zhang, *Adv. Mater.* **2022**, *34*, 2105120.

[140] P. Chen, Q. Wang, X. Wan, M. Yang, C. Liu, C. Xu, B. Hu, J. Feng, Z. Luo, *Nano Energy* **2021**, *89*, 106327.

Pei Zhang is currently pursuing her Ph.D. at the Southern University of Science and Technology. She obtained her Master's and Bachelor's degrees in Materials Science and Engineering from Zhengzhou University in 2019 and 2017, respectively. Her research is focused on the development of 3D printed flexible interactive displays for human-machine interfacing.

Yifan Yang is currently a Ph.D. student in Biomedical Engineering at South China University of Technology (SCUT). She earned her Bachelor's degree in Pharmacy from Jilin University in 2018 and her Master's degree in Biology and Medicine from Shandong University in 2023. Her research primarily focuses on electrochemical biosensing and biointerfacing.

**ADVANCED
SCIENCE NEWS**

www.advancedsciencenews.com

**ADVANCED
FUNCTIONAL
MATERIALS**

www.afm-journal.de

Zhaobo Li is now a Ph.D. candidate in the School of Biomedical Sciences and Engineering at South China University of Technology (Guangzhou International Campus, China). He received his M.Eng. degree from Xinjiang University in 2020 and worked as a junior researcher in Jihua laboratory (Foshan, China) until 2023. His current research interests focus on wearable/flexible biomedical sensing, especially in the field of brain-computer interface applications.

Xuetao Shi is a Professor at the School of Materials Science and Engineering, South China University of Technology (SCUT). He completed his Ph.D. at SCUT in 2010 and subsequently pursued postdoctoral research and served as an Assistant Professor at Tohoku University, Japan, from 2010 to 2015. His research focuses on tissue engineering and regenerative medicine, biomaterials for medical applications, and bio-3D printing technologies.

Kai Wu is a Professor in the School of Biomedical Sciences and Engineering at South China University of Technology (Guangzhou International Campus, China). He received his M.D. degree from Tohoku University (Sendai, Japan). His research interests are in a wide range of in Intelligent medical devices, medical artificial intelligence, brain science and brain diseases, *etc*.

Ji Liu is currently an Associate Professor in the Department of Mechanical and Energy Engineering, Southern University of Science and Technology. He obtained his PhD from the University of Liege (Belgium) and University of Bordeaux (France) under the framework of Erasmus Mundus Joint PhD program. Prior to joining SUStech, he conducted post-doc research in the University of Cambridge, Massachusetts Institute of Technology and Harvard Medical School. His research interest is to design and fabricate functional hydrogels and hydrogels-based electronics for biointerfacing.